MONOGRAFIAS DE FÍSICA

VIII

LOW ENERGY NUCLEAR PHYSICS
Interaction of γ-rays with nuclei

by

J. Goldemberg and A. O. Hanson

Lectures at the Latin American School of Physics
June 27 - August 7, 1960

Topics of Lectures

J. Goldemberg	I.	Introduction.
	II.	Methods of investigation.
	III.	Information on yields and cross-sections.
	IV.	Energy spectrum and angular distributions.
A. O. Hanson	V.	Elastic and inelastic scattering.
	VI.	Polarized bremsstrahlung.

Notes by: R. E. Ballestero
S. Mayo
F. Tagliabue
A. Trier

CENTRO BRASILEIRO DE PESQUISAS FÍSICAS
Av. Wenceslau Braz, 71
RIO DE JANEIRO
1960

I N D E X

I. Introduction. 1

The giant resonance. The interaction of γ-rays of energies up to 30 Mev with nuclei.

II. Methods of Investigation. 7

Residual activity. Inverse reactions (detailed balance). Electron desintegration. Inelastic electron scattering. Absorption measurements.

III. Information of Yields and Cross-Sections Competition. 26

Experimental results on photonuclear cross-sections. Properties of the giant resonance. The model of Goldhaber and Teller. Statistical model for photonuclear reactions. Typical particle yields of photonuclear reactions at 22 MeV betatron energy.

IV. Energy Spectrum and Angular Distributions. 36

Courant's model. Wilkinson's model.

V. Elastic Scattering. 44

Elastic scattering in the giant resonance region. Scattering of gamma rays in the energy region below the neutron threshold. The self-absorption experiment. The production experiment. Integrated scattering cross section.

VI. Polarized Bremsstrahlung. 57

* * *

LOW ENERGY NUCLEAR PHYSICS

I. INTRODUCTION

1) The Giant Resonance

It is perhaps interesting to introduce the subject of the interaction of γ rays with nuclei, talking about what is called the "giant resonance".

When the nuclei are bombarded by γ rays of energy from 10 to 30 Mev, the cross section for absorption of the γ rays varies with the energy like a gigantic resonance, of the order of 5 Mev wide. The giant resonance occurs whatever is the product of the reaction; this means that the shape of the cross section is a characteristic of the process of absorption of the γ rays and therefore independent of the competition of the different photonuclear reaction. Some typical curves for (γ, n) reactions are given here in fig. 1 from the data of Montalbetti, Katz and Goldemberg (P. R. 91, 659 (1953)).

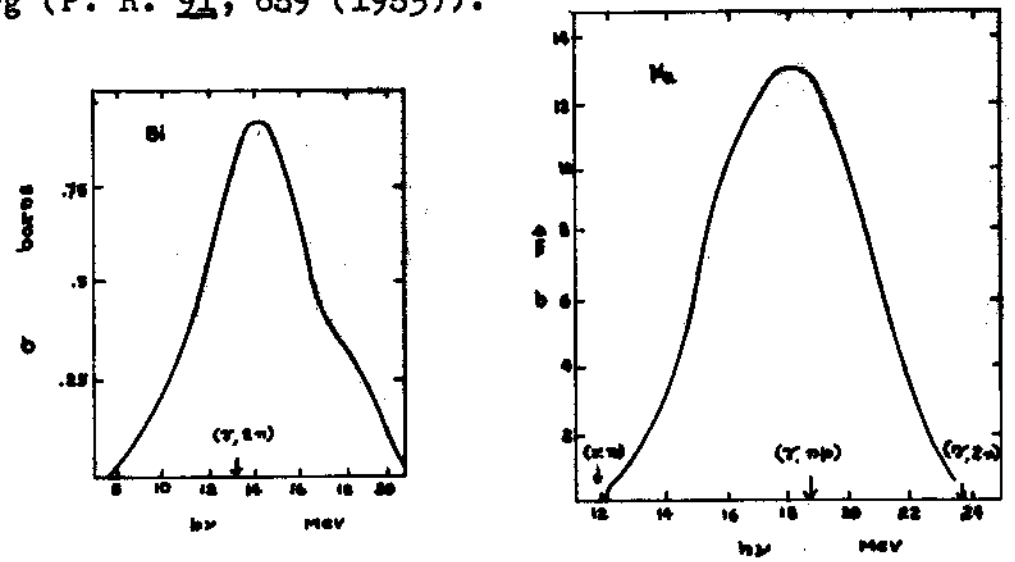

Fig. 1

2) The Interaction of γ Rays of Energies up to 30 Mev With Nuclei

Using the de Broglie's relation, the wave length of a γ ray can be written as

$$\lambda = \frac{h}{p} = \frac{1{,}25 \cdot 10^{-10}\text{cm}}{E\ (\text{Mev})}$$

For $E \sim 20$ Mev λ will be $\sim 10^{-11}$cm $\therefore$ λ is of the order of magnitude of the nucleus (Ex. for $A \sim 200$, $R \sim 10^{-12}$cm), therefore, at low energies, the interaction should not depend on the detailed structure of the nucleus which acts as "a small boat in a big wave". The effect of the electromagnetic wave should be to displace the center of mass of the protons relative to the neutrons. In the C.M. system, in a first approximation, the nucleus would be have like a dipole, and, it can be shown, |Bethe, R.M.P. 9, 87 (1937)| that protons and neutrons present an effective charge

$$e_p = \frac{N}{A}\ e$$

$$e_n = -\frac{Z}{A}\ e$$

If the nucleus was to consist of one type of particles e.g. only p or only d or only α we are going to show that no El radiation could be absorbed:

The matrix element for the transition from a state a to state b, taking the photon as a plane wave polarized in the x-direction with a propagation vector $\vec{k}$ is

$$D_{ab} = \sum_i^A \frac{e_i}{m_i} \int \psi_b^* \, e^{i\vec{k}\cdot\vec{r}_i} \, \frac{\partial}{\partial x_i} \, \psi_a \, d\tau$$

where $\vec{r}_i$ is the position of the i^{th} nucleon and the integral is extended over all space.

For $E_\gamma \sim 10$ Mev $\qquad k = \frac{2\pi}{\lambda} = \frac{2\pi}{10^{-11}} \sim 10^{10}\ cm^{-1}$

For $r_i \sim 10^{-12}$cm $\qquad \vec{k}.\vec{r} \sim 10^{-2}$ and we can write D_{ab}, in a first approximation, as

$$D_{ab} = \sum_i \frac{e_i}{m_i} \int \psi_b^* \frac{\partial}{\partial x_i} \psi_a \, d\tau$$

In the C.M. system

$$\sum_i \frac{e_i}{m_i} \frac{\partial}{\partial x_i} \psi_a = \sum_i \left(\frac{e_i}{m_i} - \frac{\sum_i e_j}{M} \right) \frac{\partial}{\partial \xi_i} \psi_a$$

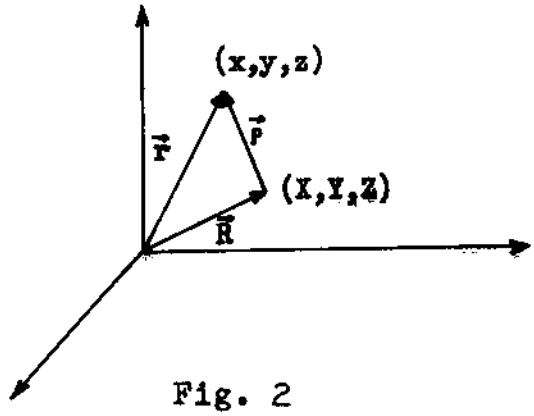

Fig. 2

where $\xi_i = x_i - X$

and X is the C.M. coordinate

$\vec{\rho} = (\xi, \eta, \zeta)$

$$\vec{R} = \sum_j \frac{m_j r_j}{M}$$

From this we can see that if the specific charge

$$e_i = \frac{\sum_i e_i}{A}$$

of all the particles is the same, the matrix element will vanish. This is true if the nuclei were formed only of p or d or α etc. and then, for these nuclei, no El absorption could take place.

a) $E_\gamma < 15$ Mev.

This is not the real case, but for low γ energies (up to $\sim$ 10 Mev) the strong correlations between the nucleons reduce the E 1 transition probability. At higher energies the correlations are destroyed and, as experiment shows, there is a high cross section explained as an E 1 absorption.

Blatt-Weisskopf gives an estimate, using the "independent particle model" for the absorption cross section for multipoles of order ℓ and photon energies $\leq$ 15 Mev.

For electric radiation of order $\ell \geq 2$ the cross section is

$$\sigma_{c\ell}\ (E_\gamma) \simeq 18\ \pi^2\ \frac{(\ell+1)\ (2\ell+1)}{\ell(\ell+3)^2\left[(2\ell+1)!!\right]^2}\ \cdot\ \frac{e^2}{\hbar c}\ \cdot\ \frac{\hbar\omega}{D_o}\ \cdot\ (k\ R)^{2\ell-2}\ \cdot\ R^2$$

where D_o is the level distance between the "low-lying" states.

This equation may not apply to electric dipole absorption because of the strong correlation between nucleons.

The absorption cross section for M ℓ radiation is smaller than the given above by the factor $10\ \hbar^2/(Mc.R)^2$.

According to this approximation the main contribution to the γ-ray absorption cross section for $\hbar\omega \leq$ 15 Mev probably comes from the M 1 and E 2 absorption only. The above estimate gives for $\hbar\omega$ = 15 Mev.

for M 1 $\quad \sigma_{c\ell}(E_\gamma) \simeq 4{,}8 \times 15\ (\text{Mev})\ .\ 10^{-4}$ barns

$$\simeq 7 \times 10^{-3} \text{ barns}$$

for E 2 $\quad \sigma_{cl}(E_\gamma) \sim 1{,}2 \times 15^3$ (Mev) . $\left(\frac{R}{6.10^{-13}\text{cm}} \right)$. 10^{-6} barns

$$\simeq 27 \times 10^{-3} \text{ barns (for A = 200)}$$

So M 1 and E 2 absorption are of the same order of magnitude for $\hbar\omega \sim 15$ Mev. and too small to explain the giant resonance.

b) $E_\gamma > 15$ Mev - The giant resonance.

Baldwin and Klaiber [P. R. 71, 3 (1947)] measured the giant resonance for $\hbar\omega > 15$ Mev and found that the integrated cross section is $\sim$ 1 Mev. barn concentrated in a region of $\sim$ 5 Mev; so the experimental value of σ is $\sim$ 0.2 barns, off by a factor 10 from the above estimates. The cross section of the giant resonance must be due to E 1 radiation. This can be justified by the simple calculation done by Levinger and Bethe [P. R. 78, 115 (1950)] for the integrated cross section for E 1 transitions using the Thomas - Reiche - Kuhn sum rule [Bethe, Handbuch der Physik 24 434].

The oscilator strength for a photoelectric dipole transition between state 0 and state n is:

$$f_{on} = \frac{2M\,(E_n - E_o)}{\hbar^2} \left| \int \psi_o^* \, z \, \psi_n \, d\tau \right|^2$$

where z is the component of the displacement along the direction of polarization of the photon. The photoelectric cross section of absorption of a photon of energy $E_n - E_o$ is

$$\sigma_{on}\,(El) = \frac{2\pi^2\, e^2\, \hbar}{Mc}\; f_{on}$$

Summing over n

$$\int \sigma dE = \sum_n \sigma_{on} = \frac{2\pi^2\, \hbar}{Mc} \sum_n e^2\, f_{on}$$

For the case of electrons in a atom it can be shown that $\sum_n e^2 f_{on} = e^2 Z$; for nuclei the introduction of the effective charge makes $\sum_n e^2 f_{on} = e^2 \frac{N.Z}{A}$ thus for the case $N = Z = \frac{A}{2}$

$$\int \sigma dE = \sum_n \sigma_{on} = \frac{\pi^2\, e^2\, \hbar\, A}{2Mc} = 0{,}015\, A \text{ Mev. barn}$$

If exchange forces are taken into account

$$\int \sigma dE = 0{,}015\; A\; [1 + 0{,}8\; x]$$

where x is the fraction of exchange forces, relative to the entire force between proton and neutron: $x \sim 0{,}55$. For $A \sim 100$ the integrated cross section is $\sim$ 1 Mev barn, in agreement with experiment. This calculation explains the integrated cross section of the giant resonance using only E 1 transitions. However, we still have to explain why all this cross section is concentrated in a narrow energy region ($\Gamma \sim 3$ to 7 Mev) and in order to do this we will have to use a nuclear model.

Before doing this let us become more familiar with the experimental results on the giant resonance.

::*:*:*:*:*

II. METHODS OF INVESTIGATION

The main techniques are the following:

a) Residual activity

b) Inverse reactions (detailed balance)

c) Electron desintegration

d) Inelastic electron scattering

e) Absorption measurements

a) Residual activity (γ, x) where x is a n (neutron) or p (proton) or d (deuteron) or γ or γ' or α or 2n etc.

Normally the n is favoured over the other emissions because of the inexistence of the Coulomb barrier. In this method one measures the total cross sections for a particular reaction measuring the activity of the residual nucleus. The rays come from a betatron or a sinchrotron or another machine; they have therefore a continuous spectrum. A rough representation of their energy distribution being:

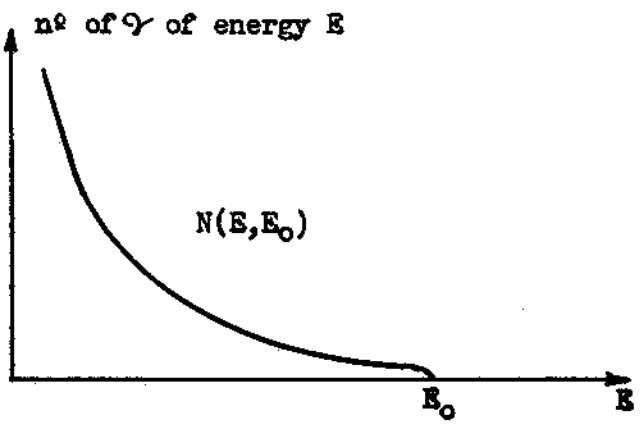

$$N(E,E_0) \propto \frac{1}{E}$$

where E_0 is the maximum energy of the spectrum.

1) How to calculate the absolute cross section

The observed number of reactions (γ, x) will be

$$\alpha(E_o) = K \int_0^{E_o} N(E,E_o)\, \sigma(E)\, d\,E \qquad (1)$$

It is an integral equation; $\alpha(E_o)$ is called the activation function and it has the shape of fig. 3; points are obtained by varying E_o. To normalize the incident number of photons an ionization chamber calibrated with a calorimeter is used. The solution of equation (1) depends on knowing $N(E, E_o)$. Fig. 4 represents the energy distribution of photons for different values of E_o normalized to 100 "roentgens" and fig. 5 gives the number of photons per indicated energy interval per 100 "roentgens" as a function of the maximum photon energy of the betatron. Now looking to curves 3 and 5 and supposing that fig. 6 represents the cross section curve we can write

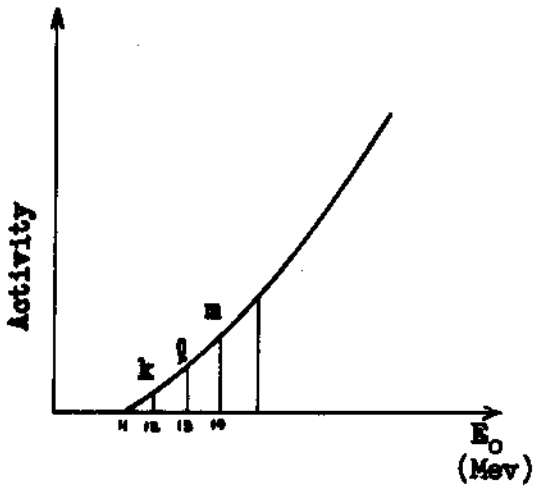

Fig. 3

$$k = \sigma_1 a_1$$

$$l = \sigma_1 a_2 + \sigma_2 b_1$$

$$m = \sigma_1 a_3 + \sigma_2 b_2 + \sigma_3 c_1$$

etc.

These linear equations can be solved for the unknowns σ_1 yielding the desired cross section curves [Johns, Katz et

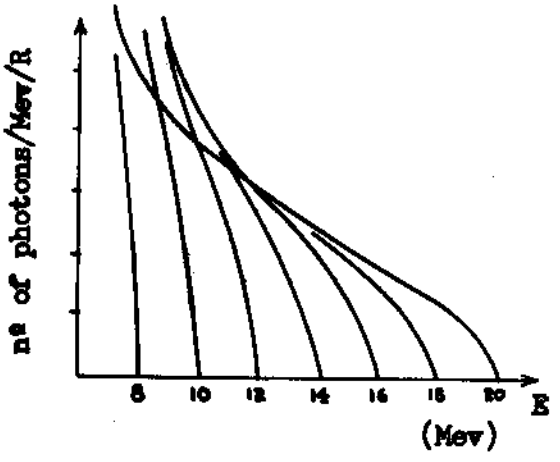

Fig. 4

al, P.R. 80, 1062 (1950)]. The method is complicated by experimental errors in k, l, m ... of the order of 2%. Because the computation involves the difference of two numbers of nearly the same magnitude, the error in some values of σ may be 50%.

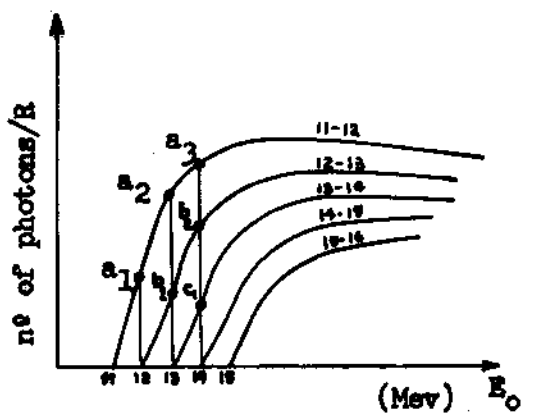

Fig. 5

A more sophisticated method of solving the problem is the "photon difference method" [Katz, Cameron-Can. J. of. Physics 1951].

b) The principle of detailed balance enables us to get the cross section of the reaction (γ,x) from the inverse reaction (x,γ) [Blatt, Weisskopf].

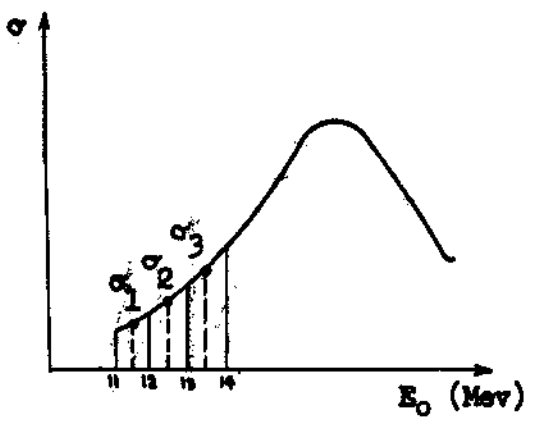

Fig. 6

It can be shown that

$$\frac{\sigma(\gamma,x)}{\sigma(x,\gamma)} = \left[\frac{k_x}{k_\gamma}\right]^2 \cdot \frac{(2s+1)\,(2j+1)}{2.\,(2j'+1)}$$

where s = spin of particle x, j = total angular momentum of the final state, j' = total angular momentum of the initial state. Since the particle energy (generally p) can be defined very well, these experiments can be done with a good resolution. Blair [P.R. 100, 21 (1955)] measured the cross section for the B^{11} (p,γ) C^{12} reaction and the result is

in very good agreement with the one obtained by Cohen [P.R. 104, 108 (1956)] for the C^{12} (γ,p) B^{11} reaction. In this reaction the transitions going to the ground state of B^{11} were measured: Fig. 7.

Unfortunately this cannot be done for all the elements, because most of the products of the (x,γ) reactions are not stable.

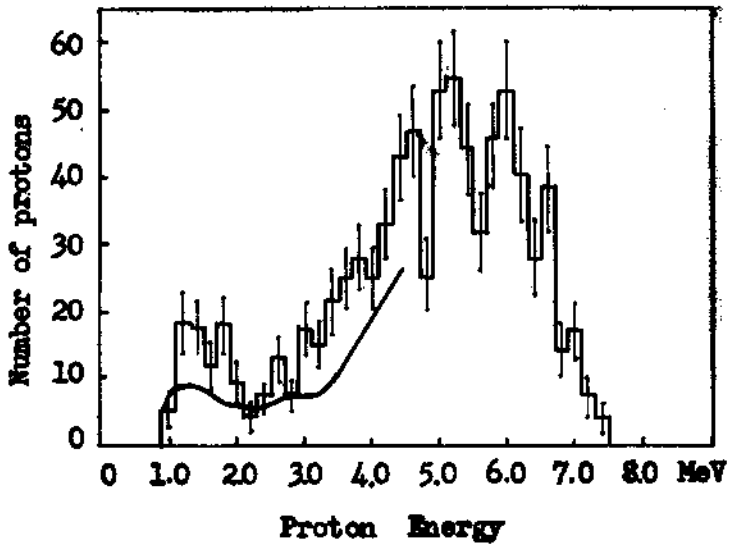

Fig. 7

c) (e,x) Reactions

(γ,x) reactions cannot be measured using monochromatic γ-ray beams (except for a few cases) due to the continuous spectrum of the bremsstrahlung. Besides that, the methods of monitoring x-rays are very unprecise. This last difficulty can be avoided using a mono-energetic electron beam to perform (e,x) reactions.

These reactions can be considered proceeding by two main contributions:

1) An electron in movement has an associated electromagnetic field which can interact with the bombarded target nucleus producing its disintegration.

2) The bremsstrahlung continuous spectrum which is produced by the interaction of the electron with the first layers of the target material is responsible for photodisintegration of target nucleus.

If a stack of thin foils is bombarded by a collimated, monoenergetic electron beam, (Skaggs et al: Phys. Rev. 73, 420 (1948)), it can be proved that the activity induced in the foils by bremsstrahlung effect is in principle, independent of the foil position. Assuming forward production of bremsstrahlung the activity induced by this effect in foil number n is a linear function of the number (n-1) of foils in front of it (Fig. 8).

On the other hand, the activity due to the associated electromagnetic field of the electron beam is independent of the foil number.

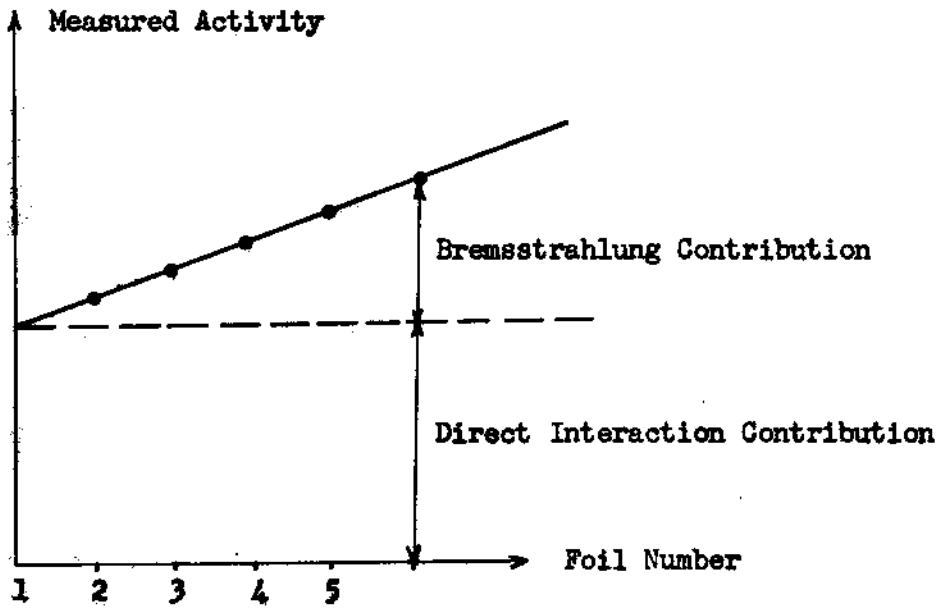

Fig. 8

It is interesting to note also that (e,x) experiments give more accurate results since there is no problem in monitoring an electron beam.

Let $(A_n)_{el}$ be the activity in foil number n due to electromagnetic or direct interaction effect, and $(A_n)_{br}$ the activity due to bremsstrahlung; then we have:

$$(A_n)_{el} = D \int_{a_{(n-1)}}^{a_n} \sum_j (\sigma_j)_{el}\, dx = D \sum_j (\sigma_j)_{el} \int_{a_{(n-1)}}^{a_n} dx$$

$$(A_n)_{el} = a\ D \sum_j (\sigma_j)_{el}$$

$$(A_n)_{br} = D \int_{a_{(n-1)}}^{a_n} \sum_j (\sigma_j)_{br}\ dx$$

where D is the intensity of the incident electron beam; a is the foil thickness $(\sigma_j)_{el}$, $(\sigma_j)_{br}$ are cross-sections for direct interaction and bremsstrahlung contributions to the (e,x) process when the target nucleus is raised to a particular excited state j.

Up to this point we already made the following main assumptions:

1º) There exists a discrete set of states $\{j\}$ for the target nucleus once excited by the electron beam.

2º) $(\sigma_j)_{el}$ is independent of the foil number provided the energy and the intensity of the incident electron beam is not appreciably reduced. This is true for electron energies high enough.

3º) The intensity of the high energy region of the bremsstrahlung spectrum is not appreciably affected by atomic interactions. The region above the (γ, x) threshold is the only one considered here; there is little backward bremsstrahlung production.

4º) $(\sigma_j)_{br}$ depends on target nucleus since it involves the properties of the foils ahead.

Now, our problem is to evaluate $(\sigma)_{el}$ and $(\sigma)_{br}$ corresponding to all possible j - final states.

To do this we have to consider the principal ways in which electromagnetic interaction could proceed; i.e. electric dipole, magnetic dipole and electric quadrupole interactions.

We proceed by two different ways to evaluate this interactions, i.e. by using Møller potentials to represent the field of the electrons at the nucleus, and by using the Weizsacker Williams approximate method to calculate the virtual quanta spectrum associated to the incident electron beam.

Let us consider first the electric dipole interactions of the incident electron beam with nuclei in the target.

Evaluation of direct interaction cross section by using Møller potentials: (Møller: Zeit. f. Physik 70 786 (1931).

Let Z be the atomic number in the target; N the number of atoms per cubic centimeter; D, as above, the intensity of incident electron beam on the target.

The transition rate for electromagnetic disintegration is

given by:

$$W_{el} = \frac{2\pi}{\hbar} \left| H'_{fo} \right|^2 G \rho_f$$

where $\rho_f = \frac{1}{8\pi^3} \frac{k_f \omega_f}{\hbar c^2} d\Omega_f$ is the density of excited nucleus final states f; $d\Omega_f$ is the solid angle element for the outgoing electron; G is the probability that the excited state will decay by nucleon emission. This probability is independent of the way in which the excited state is formed; H'_{fo} is the perturbing Hamiltonian raising the initial (ground) state of the nucleus to an excited (final) state f.

The perturbing Hamiltonian for the nucleus is

$$H' = \sum_{\nu} \left\{ - \frac{e}{Mc} \bar{A}_\nu \cdot \bar{p}_\nu + e \phi_\nu \right\}$$

where $\bar{A}_\nu$, ϕ_ν are the vector and scalar potentials evaluated over the ν protons in the nucleus; M is a nucleon mass; p is the momentum operator.

We can use Møller potentials to compute this Hamiltonian.

$$\bar{A} = 4\pi e \frac{e^{i\bar{K}\cdot\bar{r}} \vec{a}_f \bar{\alpha} \vec{a}_o}{\bar{K}^2 - \left(\frac{\omega_o - \omega_f}{c}\right)^2}$$

$$\phi = - 4\pi e \frac{e^{i\bar{K}\cdot\bar{r}} \vec{a}_f \vec{a}_o}{\bar{K}^2 - \left(\frac{\omega_o - \omega_f}{c}\right)^2}$$

where $\bar{K} = \bar{K}_o - \bar{K}_f$ is the momentum transfered to the nucleus; $\vec{a}$ is the four-component Dirac wave function for a free electron; $\bar{\alpha}$ represents the three 4×4 Dirac hermitian matrices which are

independent of $\vec{r}$, t, $\vec{p}$ and E, ω_o, ω_f are the frequencies associated to the electron before and after the interaction. Experiments at 10-20 Mev indicate that the wave function of the bombarding electron near the target nucleus are only moderately modified from a plane wave.

By putting this expressions into the Hamiltonian and making the approximation $e^{i\bar{K}\cdot\bar{r}} \cong 1 + i\bar{K}\bar{r} + \ldots$ we obtain the Hamiltonian for each particle ν whose vector position is r_ν.

$$H'_\nu = \frac{-4\pi e^2 c^2}{c^2K^2-(\omega_o-\omega_f)^2} \left\{ \frac{\hbar}{iMc} \left(\vec{a}_f \,\vec{\alpha}\, \vec{a}_o\right) \cdot \frac{\bar{\delta}}{\delta \bar{r}_\nu} + \left(\vec{a}_f\, \vec{a}_o\right) + \right.$$

$$\left. + \left(\bar{K}.\bar{r}_\nu\right) \frac{\hbar}{Mc} \left(\vec{a}_f \,\vec{\alpha}\, \vec{a}_o\right) \cdot \frac{\bar{\delta}}{\delta r_\nu} + i \left(\bar{K}.\bar{r}_\nu\right) \left(\vec{a}_f\, \vec{a}_o\right) \right\}$$

To compute the electric dipole approximation we consider the orthogonality between initial and final wave functions: $(u_f, u_o) = 0$.

We define

$$\bar{R}_\nu = \int u_f^* \, r_\nu \, u_o \, dr_\nu \quad ; \quad \bar{R} = \sum_\nu \bar{R}_\nu$$

$$\langle u_f \left|\frac{\bar{\delta}}{\delta r_\nu}\right| u_o\rangle = \frac{i}{\hbar} \langle u_f \left|\bar{p}_\nu\right| u_o\rangle = \frac{iM}{\hbar}\langle u_f \left|\frac{d\bar{r}_\nu}{dt}\right| u_o\rangle =$$

$$= \frac{iM}{\hbar} \frac{d}{dt} \left\{\langle u_f \left|\bar{r}_\nu\right| u_o\rangle\right\}$$

From the relation:

$$\frac{d\bar{r}_\nu}{dt} = \left[\bar{r}_\nu, H\right] + \frac{\delta r_\nu}{\delta t}$$

Since

$$\left[\bar{r}_\nu, H\right] = 0 \;\therefore \langle u_f \left|\frac{\bar{\delta}}{\delta r_\nu}\right| u_o\rangle = \frac{iM}{\hbar} \frac{\partial}{\delta t} \left\{\langle u_f \left|\bar{r}_\nu\right| u_o\rangle\right\}$$

$$u_o = \psi_o(r)\, e^{-i\omega_o t} \qquad u_f = \psi_f(r)\, e^{-i\omega_f t}$$

are total nuclear wave functions before and after the interaction

$$\therefore \langle u_f \left| \frac{\bar{\delta}}{\delta r_\nu} \right| u_o \rangle = - \frac{M}{\hbar} \langle u_f | r_\nu | u_o \rangle \ (\omega_f - \omega_o)$$

Computing the interaction energy for the electric dipole transition $u_o \rightarrow u_f$ keeping only terms up to $\bar{K}.\bar{r}$.

We obtain:

$$\langle u_f | H'_\nu | u_o \rangle = - \frac{4\pi e^2 c^2}{c^2\bar{K}^2 - (\omega_o - \omega_f)^2} \left\{ \frac{i}{c} (\vec{a_f} \bar{\alpha} \vec{a_o}). \bar{R}_\nu (\omega_f - \omega_o) + i(\vec{a_f}\vec{a_o})(\bar{K}.\bar{R}_\nu) \right\}$$

Summing over all particles in the nucleus:

$$\langle u_f | H' | u_o \rangle = \frac{- 4\pi e^2 c^2 i}{c^2\bar{K}^2 - (\omega_o - \omega_f)^2} \left\{ \frac{1}{c} (\vec{a_f}\bar{\alpha}\vec{a_o}). \bar{R} \ (\omega_f - \omega_o) + (\vec{a_f}\vec{a_o})(\bar{K}.\bar{R}) \right\}$$

From this matrix element the total cross section for electromagnetic interaction can be computed

$$\sigma_{el} = \frac{4}{3} \pi \left(\frac{1}{137} \right)^2 G \bar{R}^2 \left\{ \frac{\omega_o^2 + \omega_f^2}{c^2 k_o^2} \ln \left(\frac{\omega_o \omega_f - c^2 \mu^2 + c^2 k_o k_f}{c \mu (\omega_o - \omega_f)} \right) - 2 \frac{k_f}{k_o} \right\}$$

where

$$\mu = m_o c / \hbar$$

For extreme relativistic approximation this becomes:

$$\sigma_{el} = \frac{4}{3} \pi \left(\frac{1}{137} \right)^2 G \bar{R}^2 \left\{ \frac{\omega_o^2 + \omega_f^2}{\omega_o^2} \ln \frac{2\omega_o \omega_f}{c \mu (\omega_o - \omega_f)} - 2 \frac{\omega_f}{\omega_o} \right\}$$

Evaluation of bremsstrahlung contribution to the cross section

To compute this contribution to (γ, x) cross section we use the shape of bremsstrahlung spectrum for the extreme relativistic case since $\omega_o \simeq 30 \mu c$ (Heitler: The Quantum Theory of Radiation, pag. 168, (1935)).

The integrated cross section becomes:

$$\sigma_{br} = \frac{8\pi^2}{3}\left(\frac{1}{137}\right)^2 (NZ^2 r_o^2 x)\, G\, \bar{R}^2\left(\frac{\omega_f}{\omega_o} + \frac{\omega_o}{\omega_f} - \frac{2}{3}\right)\left(2\ln\frac{2\omega_o\,\omega_f}{\mu c(\omega_o-\omega_f)} - 1\right)$$

Now we can make the relation σ_{br}/σ_{el} and define the quantity F:

$$\frac{\sigma_{br}}{\sigma_{el}} = (NZ^2 r_o^2 x)\, F = (NZ^2 r_o^2 x)\left\{\frac{2\pi\left(\frac{\omega_f}{\omega_o}\right)\left(\frac{\omega_f}{\omega_o} + \frac{\omega_o}{\omega_f} - \frac{2}{3}\right)\left(2\ln\frac{2\omega_o\,\omega_f}{\mu c(\omega_o-\omega_f)} - 1\right)}{1 + \left(\frac{\omega_f}{\omega_o}\right)^2 \ln\frac{2\omega_o\,\omega_f}{\mu c(\omega_o-\omega_f)} - 2\frac{\omega_f}{\omega_o}}\right\}$$

where r_o is the classical electron radius $e^2/m_o c^2$; x is the target thickness.

In the limit when $\omega_o \cong \omega_f$ i.e. when ω_o is large we have $F \cong \frac{8}{3}\pi$.

Let us consider now the magnetic dipole interaction in the same fashion as in the electric dipole interaction except that now the perturbing Hamiltonian for the ν_{th} particle is:

$$H'_\nu = -\frac{e\hbar}{2Mc}\left(\bar{\mu}'_\nu \cdot \bar{H}\right)$$

where $\bar{\mu}_\nu$ is the total magnetic moment of the ν_{th} particle in units of nuclear Bohr magneton.

H is the magnetic field at the ν_{th} particle.

Proceeding as above, using Møller potentials the electric and bremsstrahlung total cross sections can be evaluated:

$$\sigma_{el} = G\, r_o^2\left(\frac{m_o}{M}\right)^2\left(\frac{e^2}{m_e c^2}\right)^2 \frac{\bar{M}^2}{6}\left(\frac{k_f}{k_o}\right)\left\{\frac{1}{2} + \frac{k_o^2 + k_f^2}{\bar{K}^2 - \left(\frac{\omega_o-\omega_f}{c}\right)^2} - \frac{2\mu^2\left(\frac{\omega_o-\omega_f}{c}\right)^2}{\left[\bar{K}^2 - \left(\frac{\omega_o-\omega_f}{c}\right)^2\right]^2}\right\}$$

where $\bar{M} = \sum_{\nu} \langle u_f | \bar{\mu}_{\nu} | u_o \rangle$; M is the nucleon mass

$$\sigma_{br} = \frac{2\pi^2}{3} G\, r_o^2 \left(\frac{m_o}{M}\right)^2 (Z^2 r_o^2 N x) \left(\frac{\omega_f}{\omega_o}\right)\left(\frac{\omega_o}{\omega_f} + \frac{\omega_f}{\omega_o} - \frac{2}{3}\right)\left(2 \ln \frac{2\omega_o \omega_f}{\mu c(\omega_o - \omega_f)} - 1\right)$$

Then for magnetic dipole interaction we obtain:

$$\frac{\sigma_{br}}{\sigma_{el}} = (NZ^2 r_o^2 x)\, F = (NZ^2 r_o^2 x)\, \frac{2\pi \frac{\omega_f}{\omega_o}\left(\frac{\omega_o}{\omega_f} + \frac{\omega_f}{\omega_o} - \frac{2}{3}\right)\left(2 \ln \frac{2\omega_o \omega_f}{\mu c(\omega_o - \omega_f)} - 1\right)}{\left(1 + \left(\frac{\omega_f}{\omega_o}\right)^2\right) \ln \frac{2\omega_o \omega_f}{\mu c\,(\omega_o - \omega_f)}}$$

The expression for F in this interaction is similar to that for electric dipole interaction and for $\omega_f \cong \omega_o$ is also $F = \frac{8\pi}{3}$.

The above calculations for F can be in error by 10% or more. The errors arise from the approximations we made: i.e. the use of a plane wave solution for an electron near the nucleus and the use of the extreme relativistic assumptions.

These errors are significant at small final electron energies which is the case up to 20 Mev. Better measurements could be done at 100 Mev.

In the above treatment no account was taken of the finite size of the nucleus (Dalitz and Yennie Phys. Rev. 105, 1598 (1957)).

It can be seen that the difference between the theoretical values for dipole electric and dipole magnetic transitions is not greater than 20%. The experimental errors are smaller than this figure. However it is rather hard to decide which is the type of interaction due to mixture of different interactions.

The above treatment could be greatly simplified by the

use of Weizsacker - Williams method of virtual quanta (Heitler: The Quantum Theory of Radiation, pag. 263 (1935)).

The cross section for the direct effect is:

$$\sigma_{el}(\omega)\, d\omega = \sigma(\omega) \left\{ N(\omega)\, d\omega \right\}_{el}$$

where $\left\{ N(\omega)\, d\omega \right\}_{el}$ is the number of quanta in $d\omega$ corresponding to incident electron beam of frequency ω_o, and $\sigma(\omega)$ is the photo desintegration cross section at ω.

Now

$$\left\{ N(\omega)\, d\omega \right\}_{el} = \frac{2}{\pi} \frac{1}{137} \frac{d\omega}{\omega} \ln \left\{ g \frac{b_{max}}{b_{min}} \right\}$$

$g \cong 1$ is the interaction constant; b is the impact parameter where

$$b_{max} \cong 2\pi\gamma \frac{v_o}{\omega} \qquad \gamma = 1/(1-\beta^2)^{\frac{1}{2}}$$

since for b greater than b_{max} there is little contribution to flux of outgoing nucleons; b_{min} is the de Broglie wave length of the incoming electron beam: $b_{min} = \hbar/m_o c$

According to Williams is:

$$\left\{ N(\omega)\, d\omega \right\}_{el} = \frac{2}{\pi} \frac{1}{137} \frac{d\omega_f}{(\omega_o - \omega_f)} \ln \left\{ \frac{g\omega_o^2}{\mu c(\omega_o - \omega_f)} \right\}$$

$$\sigma_{el}(\omega)\, d\omega = \frac{2}{\pi} \frac{1}{137} \frac{d\omega_f}{(\omega_o - \omega_f)} \ln \left\{ \frac{g\omega_o^2}{\mu c(\omega_o - \omega_f)} \right\} \sigma(\omega)$$

Now to compute the bremsstrahlung contribution Williams considered the reverse system in which the electron is at rest and

subjected to the virtual quanta of the moving target nucleus. Using the Klein Nishina formula for scattering and transforming back to the direct system in which the target nucleus is at rest, it results

$$\left\{ N(\omega)\, d\omega \right\}_{br} = \frac{16}{3} \frac{r_o^2}{137} \frac{Z^2 d\omega}{\omega_o - \omega_f} \ln \left\{ \frac{q\omega_o^2}{\mu c(\omega_o - \omega_f)} \right\}$$

here $q \cong 1$ is the interaction constant in the reverse system.

$$\sigma_{br}(\omega)\, d\omega = \frac{16}{3} \cdot \frac{1}{137} (NZ^2 r_o^2 x) \frac{d\omega_f}{\omega_o - \omega_f} \ln \left\{ \frac{q\omega_o^2}{\mu c(\omega_o - \omega_f)} \right\} \sigma(\omega)$$

We then have as above

$$(Z^2 r_o^2 x N) F = \frac{\sigma_{br}(\omega)}{\sigma_{el}(\omega)} = \frac{8\pi}{3} (Z^2 r_o^2 x N) \ln (q/\varepsilon)$$

$$\therefore F \cong \frac{8\pi}{3}$$

as the result already obtained by using Møller potentials.

Let us compare now the calculated and experimental F-values when the energy of the incident electron beam is 16 Mev on target nucleus Cu^{63}; Ag^{107}; Ag^{109}.

It can be seen that by a suitable combination of the different interactions the experimental results could be explained. Other experiments have been made by Scott et al. [Phys. Rev. 100 209 (1955)] and by Barber [Phys. Rev. 111 1642 (1958)].

d) Let us consider now (e,e') experiments. With 187 Mev electrons on C^{12} it has been measured the angular distributions for the

elastic and inelastic groups (Fig. 10).

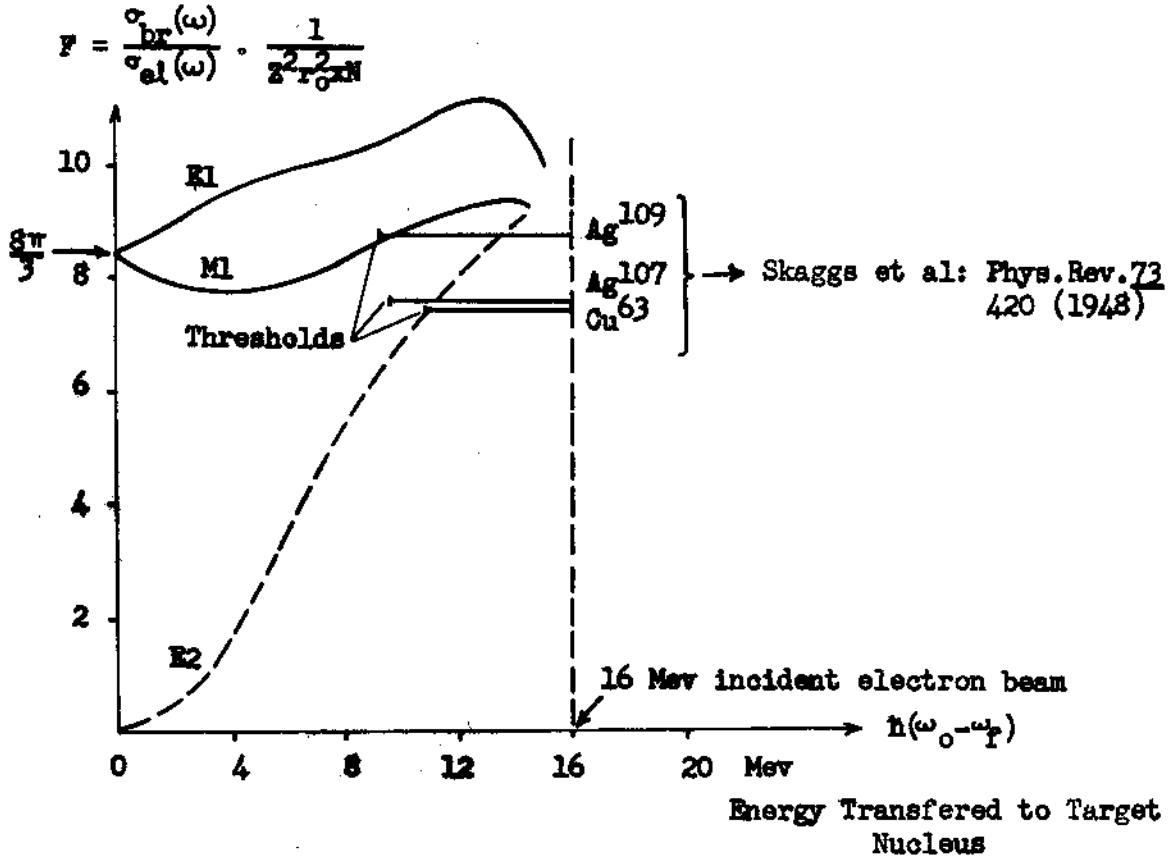

Fig. 9

The authors did also the same experiments at 80 and 150 Mev. By plotting the values at $\theta = 90^{\circ}$ for the relation $\frac{d\sigma/d\Omega(C^{12}\ 4.43\ Mev)}{d\sigma/d\Omega\ (GS)}$ as a function of bombarding energy, we obtain (Fig. 11), $\frac{d\sigma/d\Omega\,(C^{12}\ 4.43\ Mev)}{d\sigma/d\Omega\,(GS)}$.

G. Morpurgo (Nuovo Cimento X N° 3, 430 (1956)) succeeded in obtaining an expression of the above relation in C^{12} where the

$$\frac{(d\sigma/d\Omega)\ inelastic}{(d\sigma/d\Omega)\ elastic} = \frac{9}{2}\ \frac{\Lambda^2}{Z^2}\left(\frac{q^2}{q\nu}\right)^2 \Big/ \left(1 - \frac{q^2}{q\nu}\right)^2$$

coupling parameter Λ is $\cong 1$ for jj coupling and $\cong \sqrt{3}$ for LS coupling.

ν is a oscilator index wave function for the nucleus;

$q = 2 p_o \sin \frac{\theta}{2}$ where $q = \bar{p}_o - \bar{p}_f$ is the momentum transfered

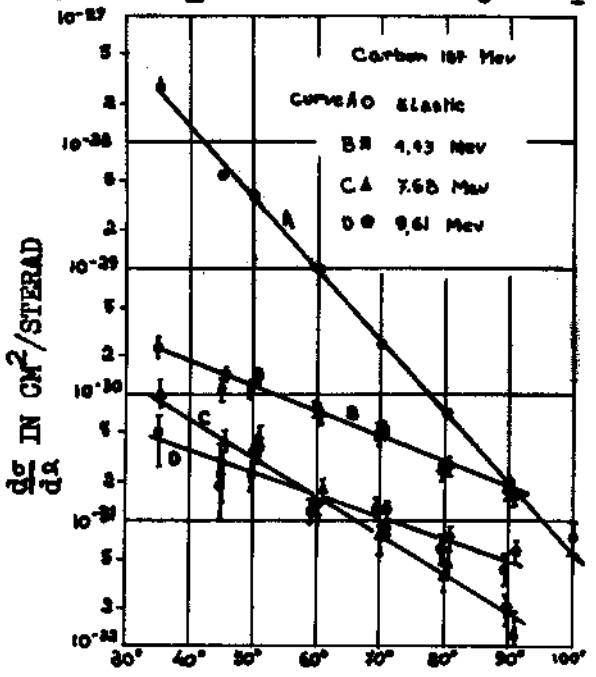

Fig. 10 (from Fregeau and Hofstadter Phys. Rev. 99, 1503 (1955)).

to the nucleus; Z is the atomic number of target nucleus. He concluded that the structure of C^{12} GS and 4.43 Mev could be

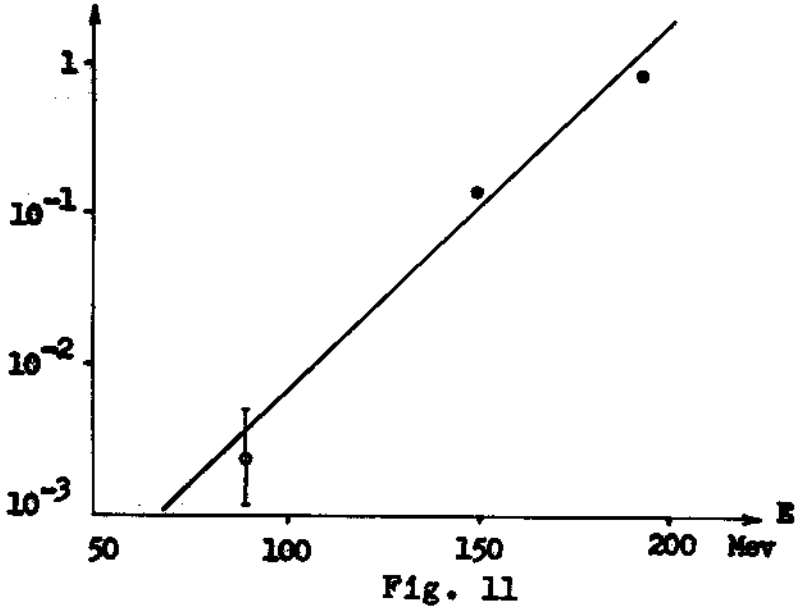

Fig. 11

described better by LS coupling wave functions. We see that this type

of experiments could give us information on nuclear structure.

e) Absorption measurements

There is another magnitude which is important when one considers the interaction of gamma rays with matter: the attenuation coefficient.

As we know the production of X-rays in a betatron gives a bremsstrahlung spectrum which makes difficult the interpretation of experiments. However there are some tricks which allow us to simplify the picture. Let us consider a bremsstrahlung continuum spectrum $N(E_o, E)$ with maximum energy E_o interacting with a nucleus to produce a (γ,x) reaction with threshold E_T such that E_o is slightly greater than E_T. This is a way to filter out the bremsstrahlung spectrum allowing it to react only with the fraction

$$E_T \leq E \leq E_o$$ (Adams et al: Phys. Rev. 74 1707 (1948))

The attenuation coefficient, as usual, is defined by:

$$I = I_o \; e^{-\mu x} \qquad \mu x = N\sigma_{tot}\, x$$

$$\sigma_{tot} = \sigma_{ph} + \sigma_c + \sigma_{pp} + \sigma_{nucl.} + \sigma_{tr}$$

where: N = number of atoms per cubic centimeter in target material; x is target thickness in cm; σ_{ph}; σ_c; σ_{pp}; $\sigma_{nucl.}$; σ_{tr} are cross sections for photoelectric, Compton, pair production, nuclear and triplet interaction effects.

As is well known:

$$\sigma_{ph} \cong \frac{Z^4}{(h\nu)^3} \; ; \quad \sigma_c \cong \frac{Z}{(h\nu)^2} \; ; \quad \sigma_{pp} \cong Z^2 \ln E \; ; \quad \sigma_{tr} \cong Z \ln E$$

Nuclear cross section is in general of the order of 5% of the total cross section, so such a measurement becomes rather hard to do. However total absorption coefficients could be measured with the aid of a NaI(Tl) crystal spectrometer.

Wyckoff and Koch (NBS6313) reported such measurement on different materials:

H, C, Al and water:

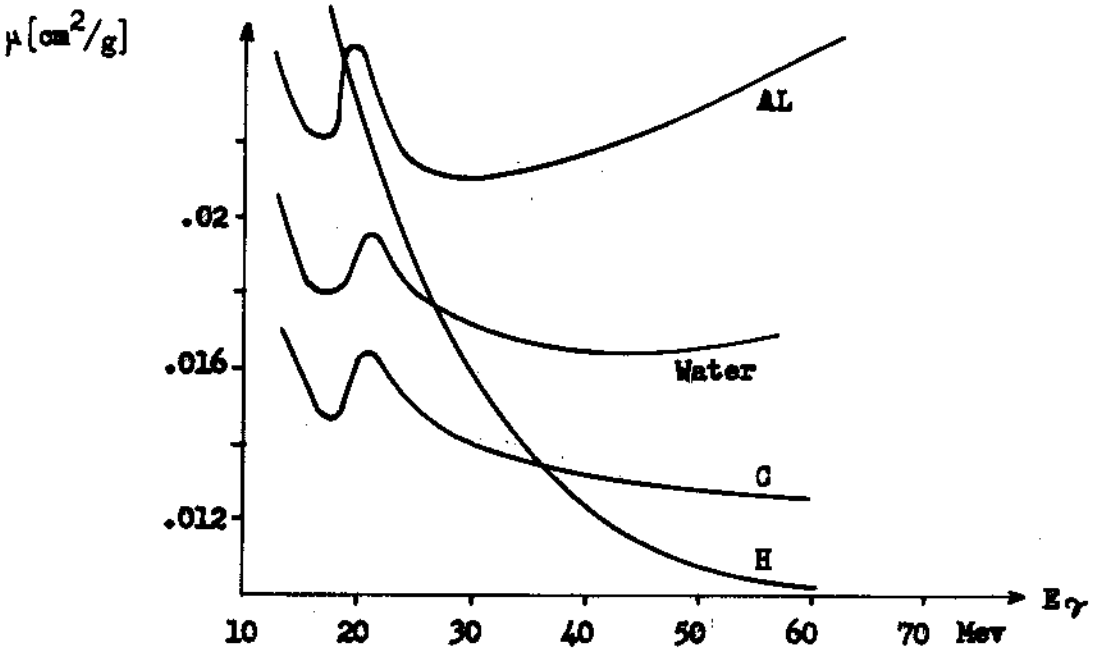

Fig. 12

A bump in the attenuation coefficient versus E_γ curve can be observed in the giant resonance region; for high gamma energies the σ_{pp} and σ_{tr} become more and more significant with increasing values of Z, (Fig. 12).

Finally we have to point out that experimental measurements of this type are not always in good agreement due to the difficulties in measuring absolute gamma interaction cross sections. The normal instruments used in this field are: total absorption scintillation spectrometer, Compton spectrometer and pair spectrometer.

::*:*:*:*:*

III. INFORMATION ON YIELDS AND CROSS-SECTIONS COMPETITION

Experimental results on photonuclear cross-sections. Properties of the giant resonance:

For a systematic account of a) the position E_m of the maximum in the cross-section; b) the maximum cross-section and c) the width Γ of the giant resonance, fig. 13, some definite nuclear model must be constructed. Several such attempts will be examined.

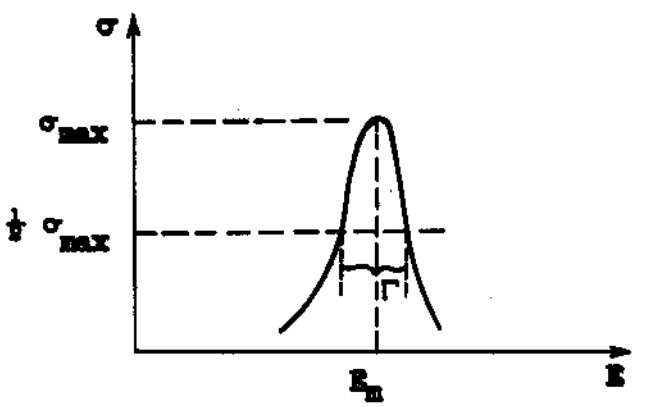

Fig. 13

Experiments covering about 40 elements were carried out in the years 1952-53 by Montalbetti, Katz and Goldemberg (Phys.Rev. 91, 659(1953)) using bremsstrahlung with a maximum betatron energy of 23 Mev. In the experiments photoneutrons were measured, giving $\sigma(\gamma,n) + \sigma(\gamma,np) + 2\sigma(\gamma,2n) \neq \sigma_{absorption}$. The integrated cross-section up to 23 Mev neglects the tail of the giant resonance, but the error involved is not expected to exceed 10%. In fig. 14 a typical plot of E_m vs. mass number A is given.

Montalbetti et al. found $E_m = 37 \times A^{-0.186}$, while Ferguson et al. found $E_m = 38.5 \times A^{-0.19}$ (Phys. Rev. 95, 776).

As will be seen, this is in good agreement with a collective model of Goldhaber and Teller. Both fits were made for about 20 elements.

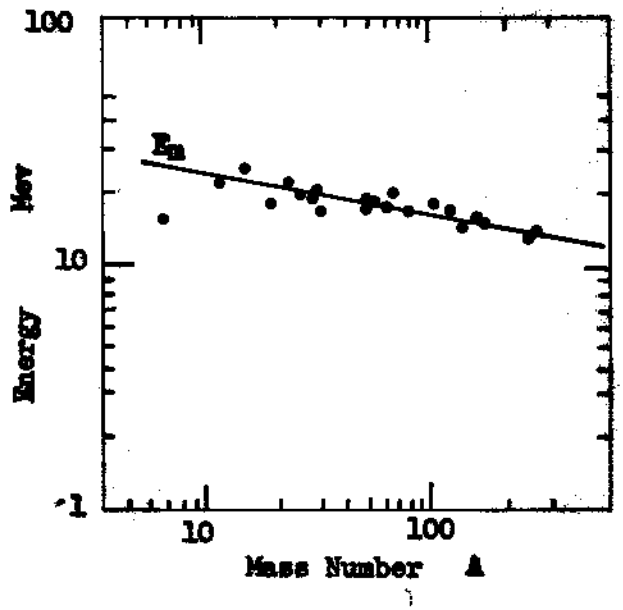

Fig. 14

Fig. 15 gives a plot of the integrated cross-section vs. A. The upper curve takes exchange forces into account using

$$\int \sigma dE = 0.015 \frac{NZ}{A}(1+0.8x), x=0.5$$

The lower curve is for x = 0 (no exchange forces). For A $\geq$ 100 the agreement with experimental results is fairly good.

At lower mass numbers the strong competition from (γ, p) reactions must be taken into account. These reactions have been systematically investigated by Weinstock and Halpern P.R. 94 1651 (1954). In fig. 16 the curve for photoproton yield as a function of Z (atomic number) is reproduced. They found that the trend of experimental data could be explained below Z = 50 using Weisskopf and Ewing's (Phys. Rev. 57, 472) statistical theory, i.e., formation of a compound nucleus and subsequent evaporation of particles. The cross sections between Z = 50 and Z = 90 are much too high, however.

We discuss now some models which have been proposed

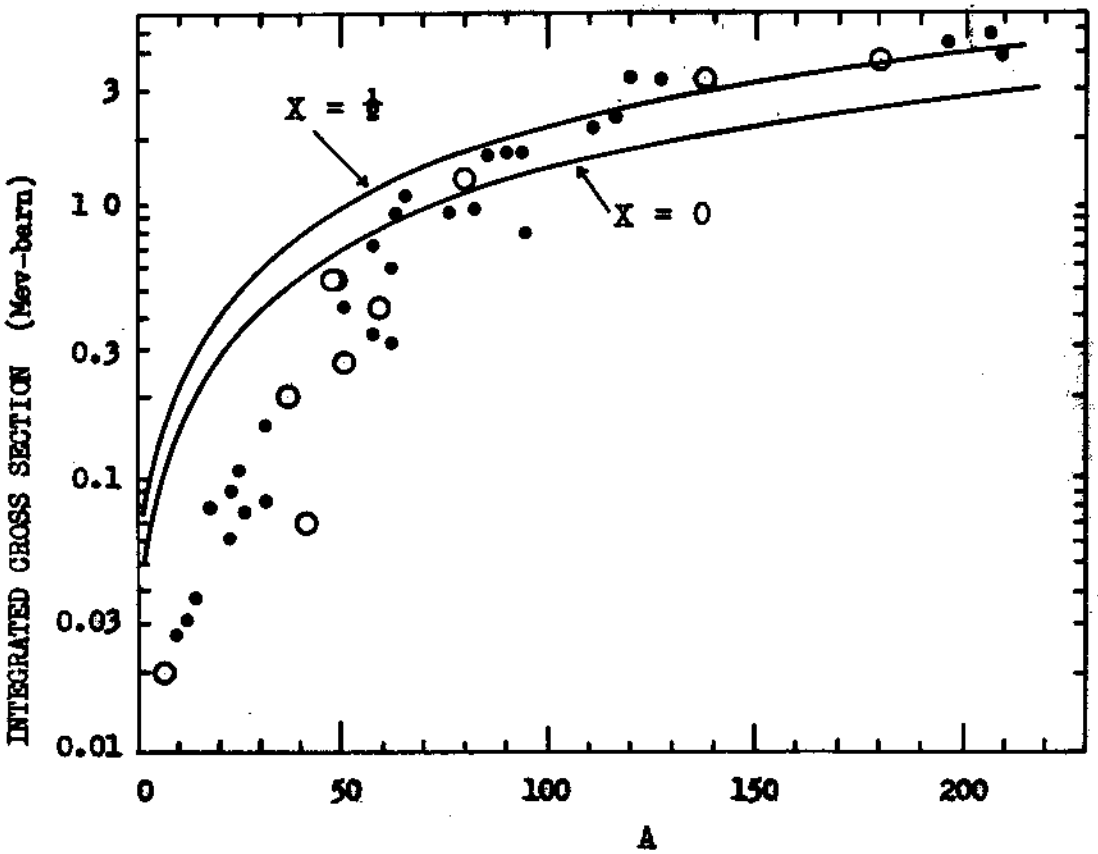

Fig. 15

to account for the behaviour of the giant resonance.

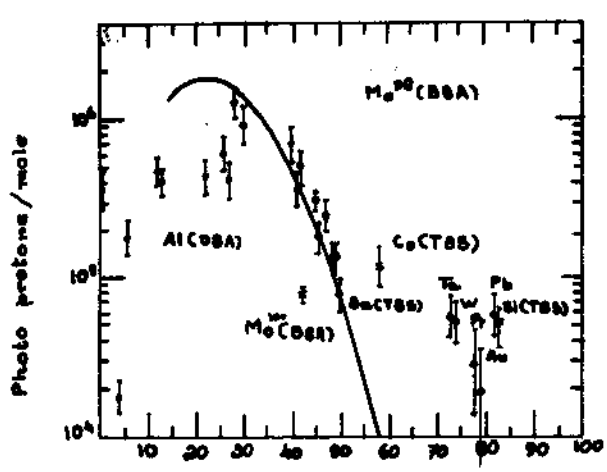

Fig. 16 Summary of published photoproton yield data. The solid curve is the yield vs Z as predicted by the calculations described in the text.

The model of Goldhaber and Teller (GT).

Assumptions - 1) Protons and neutrons inside the nucleus behave like two incompressible, interpenetrating liquids. There are as many protons as there are neutrons ($Z = N = A/2$); 2) a γ-ray incident on a nucleus displaces the protons on account of the electric field associated with it; in the C.M.C.S. the protons and the neutrons are displaced in opposite directions; 3) The restoring force acting against this displacement ξ is proportional to it as long as $\xi < \epsilon$, where ϵ is of the order of the range of nuclear forces, that is, $\epsilon \approx 2 \times 10^{-13}$cm.

The vibration thus induced is called dipole vibration. On the basis of the above assumptions a very simplified theory can be constructed, which will not account for the resonance width. (The latter may originate in a damping process due to nucleon collisions, or in a coupling of the dipole oscillation with other modes).

Let us now call ρ the proton or neutron "density" (number per unit volume) and φ the separation energy of a neutron-proton pair. If the relative displacement of the neutron and proton spheres is $\xi > \epsilon$, the total separation energy is equal to φ x number of separated nucleons. This may be crudely approximated by

$$V_{sep} = 2 \times (\pi R^2 \xi) \times \rho \times \varphi$$

R being the nuclear radius. The force is then

$$F_{sep} = - \frac{\partial V_{sep}}{\partial \xi} = - 2 \pi R^2 \rho \varphi$$

For $\xi < \epsilon$ a restoring force acts:

$F_{rest} = -k\xi$ and at $\xi = \epsilon$ we must have

$F_{rest} = F_{sep}$ giving

$$F_{rest} = -\frac{2\pi R^2 \rho\varphi}{\epsilon} \cdot \xi$$

Now

$F_{rest} = M\ddot{\xi}$ with $M = \frac{1}{2} \cdot \frac{4}{3}\pi R^3 \rho m$, where M is the reduced mass and m is the nucleon mass. (Neutrons and protons are taken with the same mass). We get the equation of S.H.M.: $\ddot{\xi} + \omega^2 \xi = 0$ with $\omega = \left(\frac{3\varphi}{\epsilon R m}\right)^{\frac{1}{2}}$.

The vibration energy $E_m = \hbar\omega = \left(\frac{3\hbar^2}{\epsilon m r_o}\right)^{\frac{1}{2}} A^{-1/6}$ using $R = r_o A^{1/3}$ and assuming the vibration energy to correspond to the position of the cross-section resonance. This $A^{-1/6}$ dependence of E_m is in fairly good agreement with the experimental results, as has already been mentioned. r_o may be taken to be 1.5×10^{-13}cm and φ, ϵ are adjusted for a detailed fit.

GT have proposed other models. One of them has been worked out by Steinwedel, Jensen and Jensen (SJJ). In this model protons and neutrons are assumed to oscillate against each other as compressible fluids, the espherical shape of the nucleus being preserved; local density fluctuations appear. Due to nuclear surface tension this model may be considered more realistic. The total nucleon density is assumed constant and the retarding forces are derived from an energy density depending on the local neutron excess.

This model gives $E_m \propto A^{-1/3}$. The resonance width would be independent of A. The experimental data on E_m vs. A seem to favor the GT model, but evidence is not conclusive.

We may summarize by writing $E_m = k\, R^{-n}$, with

$$n = 1/2 \text{ for GT}, \quad n = 1 \text{ for SJJ}$$

The additional broadening of the cross-section resonance in non-spherical nuclei may be understood qualitatively from a simple argument related to the non-sphericity of nuclei (nuclei having only filled shells are spherical). Let R_1, R_2 be the principal radii of an ellipsoidal nucleus. It will have a quadrupole moment $Q = \frac{2Z}{5}(R_1^2 - R_2^2)$. The nuclear radius "seen" by the electric field of the incident photon will be $R_2 \leqslant R \leqslant R_1$. The measured resonance then comes from a superposition of resonances spread between $E_{m_1} = k\, R_1^{-n}$ and $E_{m_2} = k\, R_2^{-n}$. Then

$$\frac{\Delta E}{E_m} = \frac{R_2^{-n} - R_1^{-n}}{R_o^{-n}}$$

If the nuclear deformation is not large, we may set $2R_o = R_1 + R_2$

$$R_2^{-n} - R_1^{-n} = \left\{ \frac{d}{dr}(R^{-n}) \right\} (R_2 - R_1)$$

$$= -n\, R_o^{(-n-1)} (R_2 - R_1)$$

$$= -\frac{n}{2}\, R_o^{(-n-2)} (R_2^2 - R_1^2)$$

Comparing with the expression for Q, it turns out that

$$\frac{\Delta E}{E} = \frac{5nQ}{4ZR_o^2}$$

For magic nuclei a narrow resonance would be expected. The trend of the measured Γ's shows this qualitatively, as may be seen from fig. 17. The trend is not as marked as with the Q's. It is to be noted that experimental errors are large.

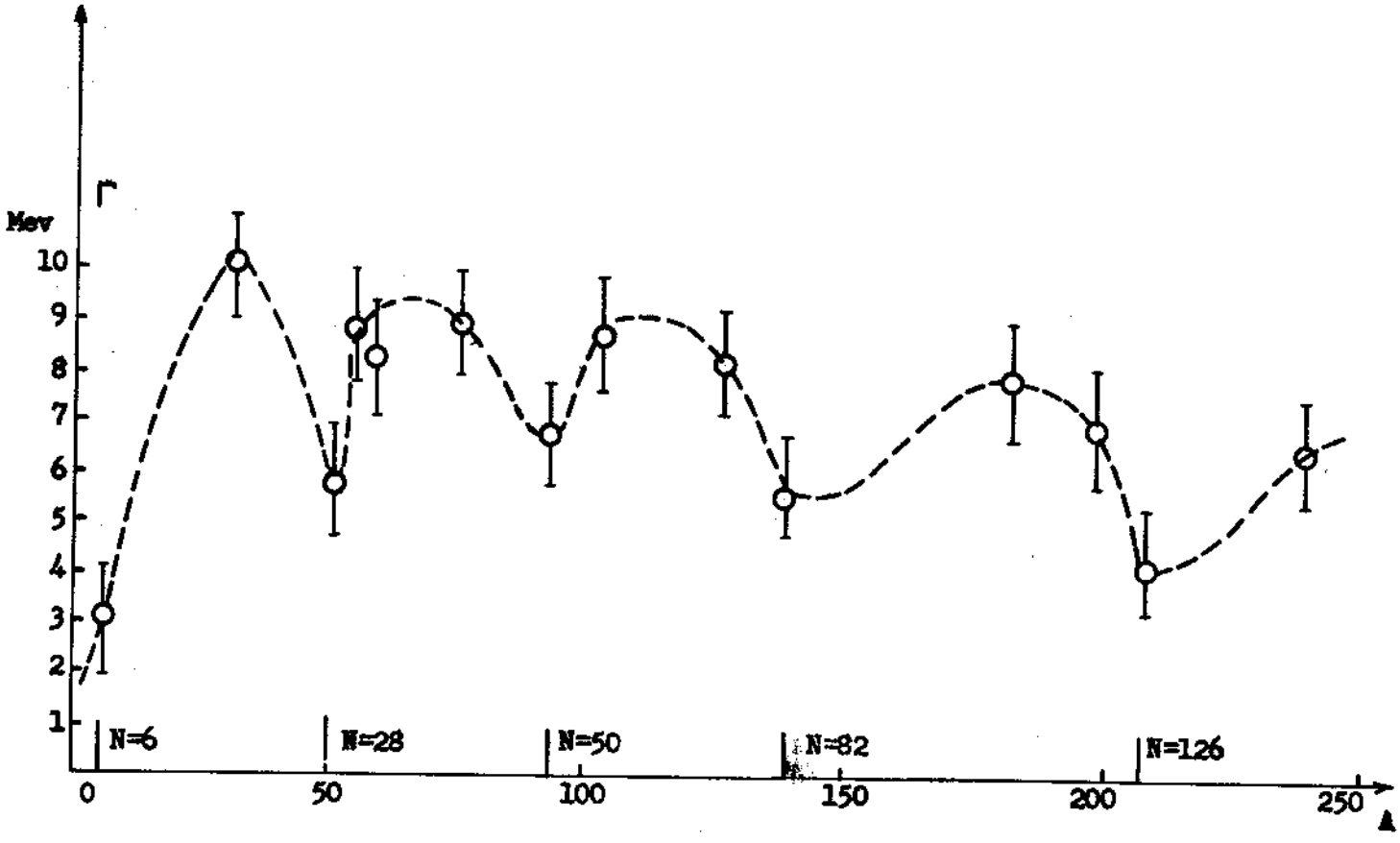

Fig. 17

A sort of splitting of the giant resonance according to the E_m values associated with the principal radius of a non-spherical nucleus might be expected, as has been shown by Danos (Nucl. Phys. 5, 23). Okamoto (Phys. Rev. 110, 143) concludes that there is a strong correlation between nuclear deformation and the resonance width of photonuclear reactions. For spherica

nuclei, the width seems to be roughly constant (4 to 5 Mev), although this may be due to competing effects. Shell effects and resonance splitting complicate the Γ vs. A dependence. A small splitting effect has actually been observed.

Wildermuth (Z.f. Naturf. 10a, 447) has tried to derive the resonance width from the SJJ model introducing damping due to neutron - proton collisions.

Statistical model for photonuclear reactions - The process of particle emission following γ-absorption may be pictured as due to a "heating up" of the nucleus through damping of the vibrations. The statistical theory of nuclear reactions is presented in Blatt and Weisskopf's treatise. Reactions are assumed to proceed through the formation of a compound nucleus:

$$\sigma(\gamma, X) = \sigma_{capt}(\gamma) \frac{\Gamma_X}{\sum_{X'} \Gamma_{X'}}$$

Here $\sigma_{capt}(\gamma)$ is the absorption cross-section for γ-rays and the Γ's are proportional to branching ratios for particle emission. The summation is over all channels of particle emission. The Γ's verify the relation:

$$\omega_c(E)\Gamma = \frac{m}{h^2\pi^2} \int_0^{\epsilon_{max}} \epsilon\, \sigma_c(E)\, \omega_R(\epsilon_{max} - \epsilon)\, d\epsilon$$

The ω's are the level densities of the compound and residual nuclei at energies E and $(\epsilon_{max} - \epsilon)$, ϵ is the energy of the emitted particle and m the reduced mass. (Energies must be calculated in the C.M.C.S.). For a calculation assumptions are

needed: a) shape and depth of nuclear potential well; b) level densities. The latter are taken to follow $\omega = Ce^{2\sqrt{aE_1}}$; here C and a are empirical values and E_1 is the excitation energy "corrected" for shell and pairing effects. See fig. 18.

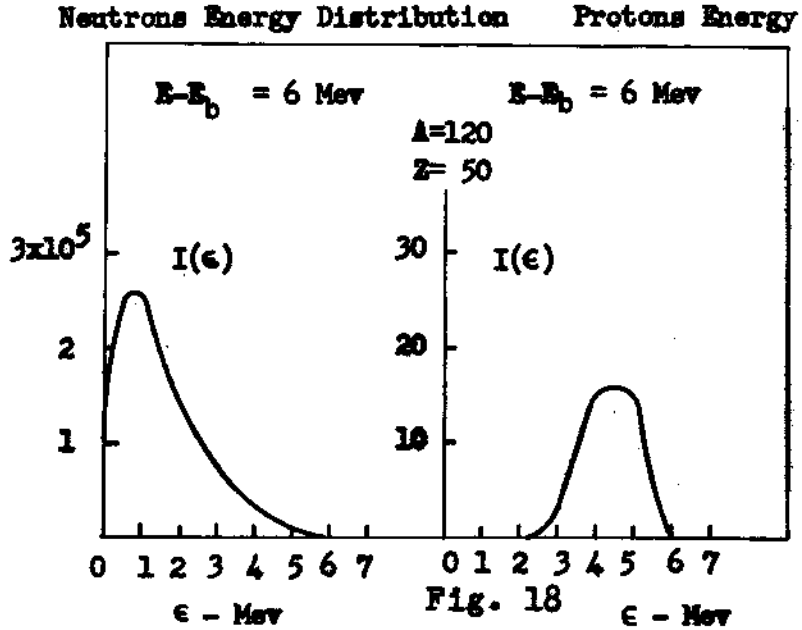

Fig. 18

Neutron emission is the favored process. If a calculation is carried out along the lines indicated above the following conclusions may be drawn:

1) 90% of the neutron emission can be accounted for by the statistical theory;

2) The ratio $\frac{\sigma(\gamma,p)}{\sigma(\gamma,n)} = \frac{\Gamma_p}{\Gamma_n}$ comes out approximately correct for the lighter elements, but is much too high for the heavier ones (by a factor of 10^2); in the latter case the angular distribution cannot be explained on the basis of evaporation.

3) The $(\gamma, 2n)$ cross-sections can be derived from the (γ, n). It is a typical evaporation process and the cross-section

may be higher than the (γ, p). The results and calculations for $\sigma(\gamma,2n)/\sigma(\gamma, n)_{tot}$ are given in figure 19. The agreement is fairly good. (Results from I.C. Nascimento, G.Moscati and J. Goldemberg at S. Paulo).

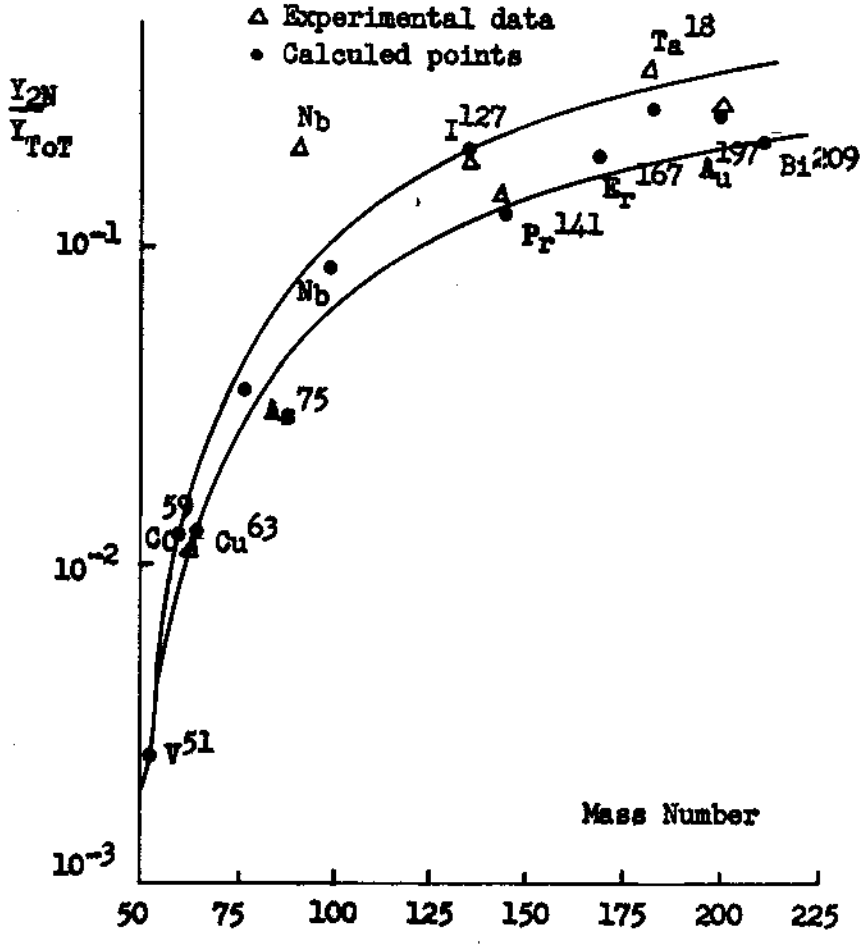

Fig. 19

Typical particle yields of photonuclear reactions at 22 Mev betatron energy

n	10^8/mol/roentgen
2n	10^7 "
p	10^6 "
d	10^5 "
α	10^4 "

IV. ENERGY SPECTRUM AND ANGULAR DISTRIBUTIONS

Looking at the angular distribution of outgoing particles from (γ,x) reactions it turns out that the neutron distribution has a maximum around 90° with a shape $a + b \sin^2 \theta$; θ is the particle scattering angle. In addition there is a fraction of high energy neutrons which cannot be eas.ly explained in terms of the evaporation model.

The proton distribution presents a broad maximum between 0° and 90° in the angular distribution and a long tail in the energy distribution. This seems to be (specially with medium and heavy weight nuclei) an indication of direct interaction process; the Coulomb barrier prevents the proton evaporation and favours neutrons evaporation. If we look at the energy spectrum of outgoing particles we observe for neutrons a maximum yield around the 1 Mev region and a long tail going up to the 10 Mev region. This tail includes 10% more neutrons than those predicted by the evaporation model.

For protons there is a Coulomb barrier and then the energy spectrum is bell-shaped going from ~ 6 to ~ 10 Mev.

If we assume that the photonuclear giant resonance, as proposed by N. Bohr, proceeds via compound nucleus formation and subsequent decay via statistical model, we must expect that 1) reaction products come out isotropically 2) the ratio between the proton and neutron yields should be particularly low (specially for heavy nuclei) 3) the neutron spectrum in the heavy ele-

ments should have an extremely low fraction of fast neutrons.

Experimental results indicate that the proton-neutron yield ratio is several orders of magnitude greater than required by evaporation theory. Fast neutrons are produced predominantly by photons in the region of giant resonance giving experimental evidence that the giant resonance can be attributed to strong individual particle transitions rather than to a collective type of photon absorption (Ferrero et al. Nuovo Cimento, Serie X, vol. 5, pag. 242 (1957)).

Courant's model (P.R. 82, 703 (1951)).

We are going to consider now the direct photodisintegration process in detail. From experiments with 17.6 Mev monochromatic gamma rays on targets with $A \simeq 100$ it turns out that $N(\gamma,p)/N(\gamma,n) \simeq 20$ to 100 times greater than the ratio predicted by the evaporation model.

However the agreement with experiments could be achieved if we consider the proton contribution as proceeding via direct interaction without formation of compound nucleus state.

Direct interaction process seems to be supported by experimental angular distribution with photoprotons emitted preferentially at 90° (Curtiss et al. P.R. 77, 290, (1950)). On the other hand Price P.R. 93 (1954) 1277 found an anisotropic angular distribution for photoneutrons, Ferrero et al. (Nuovo Cimento 4, 418) found a strong anisotropy for the photoneutrons ejected by Bi. F. Tagliabue and J. Goldemberg (to be published)

measured the angular distribution for 13 elements and found a definite anisotropy only for Bi, Au, and Pb.

Let us consider the nucleus as a square well with Z protons filling the lowest states in which each nucleon has its own independent wave function. This is supported by the fact that the mean free path of a nucleon in nuclear matter is larger than nuclear dimensions, so that we assume that even in an excited state, nucleons in the nucleus behave like individual particles with an initial wave function of the form:

$$\psi_o = A_\ell \; j_\ell (ar) \; Y_\ell^n (\theta, \phi) \qquad r < R$$

$$\psi_o = A_\ell \; \frac{j_\ell(ar)}{k_\ell(br)} \; k_\ell (br) \, Y_\ell^n (\theta, \phi) \qquad r > R$$

where $a^2 = (2M/\hbar^2)(W-|E_o|)$; $b^2 = 2M|E_o|/\hbar^2$; W is the nuclear well depth, E_o is the eigenvalue of the initial state, which can be determined by the continuity condition on the nuclear surface with radius R

$$- b \, k_{\ell-1} (bR)/k_\ell (bR) = a \, j_{\ell-1} (aR)/j_\ell(aR)$$

$Y_\ell^n (\theta,\phi)$ are spherical harmonics normalized so as to make $\int |Y_\ell^n(\theta,\phi)|^2 \, d\Omega = 1$. A_ℓ is determined by the normalization condition $\int |\psi|^2 \, dV = 1$ with spherical Bessel functions:

$$j_\ell (x) = \sqrt{\frac{\pi}{2x}} \; J_{\ell+\frac{1}{2}} (x)$$

$$n_\ell (x) = (-1)^{\ell+1} \sqrt{\frac{\pi}{2x}} \; J_{-\ell-\frac{1}{2}} (x) \qquad k_\ell(x) = \sqrt{\frac{2}{\pi x}} \; K_{\ell+\frac{1}{2}} (x)$$

The final state wave function is of the form:

$$\psi_1 = C_{\ell'}\, j_{\ell'}(cr)\, Y^{m'}_{\ell'}(\theta\,\phi) \qquad r < R$$

$$\psi_2 = C_{\ell'}\, \frac{j_{\ell'}(cR)}{Z_{\ell'}(dR)}\, Z_{\ell'}(dr)\, Y^{m'}_{\ell'}(\theta\,\phi) \qquad r > R$$

Where $c^2 = a^2 + 2M\hbar\omega/\hbar^2$; $d^2 = -b^2 + 2M\hbar\omega/\hbar^2$, $\hbar\omega$ is the energy of the absorbed quantum and $Z_{\ell'}(dr)$ is the radial part of the wave function which satisfies the continuity condition on nuclear surface:

$$d\, Z_{\ell'-1}(dR)/Z_{\ell'}(dR) = C\, j_{\ell'-1}(cR)/j_{\ell'}(cR)$$

The normalization constant $C_{\ell'}$ is chosen such that $r\,\phi_1$ is a sine wave of unit amplitude at infinity where ϕ_1 is the radial part of the wave function. Let us consider a beam of γ ray incident in the Z-direction and circularly polarized in the x + iy direction. The cross section for the dipole absorption of a photon of energy $\hbar\omega$ is:

$$\sigma = \frac{e'^2}{\hbar c}\, \frac{4\pi M\omega}{d\hbar} \int \left|\psi_0 \psi_1 \left(\frac{x+iy}{\sqrt{2}}\right) d\tau\right|^2$$

where the effective charge $e' = eN/A$ for protons.

Carrying out the integration for the matrix element for the dipole interaction of the gamma ray with one proton of angular momentum ℓ and taking the asymptotic expression of the Bessel functions we obtain:

$$\sigma = \frac{16\pi}{3}\, \frac{e'^2}{\hbar c} \left(1 - \frac{Z}{A}\right)^2 \cdot \frac{T\,W}{(\hbar\omega)^3\left\{(\hbar\omega+T)^{\frac{1}{2}}+(\hbar\omega+T-\omega)^{\frac{1}{2}}\right\}} \left\{\frac{\hbar^2}{2MR^2}\right\}^{3/2} R^2$$

Roughly $\sigma \sim \frac{1}{(\hbar\omega)^3}$.

where T is the kinetic energy of the proton in the nucleus; W is the nuclear well depth. We did not consider yet the Coulomb barrier. The actual cross section is reduced by this effect.

To fix ideas let us consider a Fermi distribution inside the nucleus; taking $\hbar\omega$ = 17.6 Mev; T_{max} = 22 Mev; W = 30 Mev; R = 1.5 × $A^{1/3}$ fermis; if we average over all possible phase α we obtain for the total cross-section:

$$\sigma = 0.044 \, (Z/A^{1/3})^2 \int_0^{x_1} P \, dx$$

where P is the penetration probability calculated from Wesskopf's penetration cross section divided by πR^2; x is the energy of outgoing protons measured in units of the barrier height; x_1 is the maximum energy of outgoing protons. The theoretical values fall short by a factor of $\sim$ 10 in respect to the experimental values.

In view of the crudeness of this model the disagreement is not surprising; however the predicted cross sections could be increased by a factor 4 is we replace the potential square well by a "wine bottle" potential suggested by Feenberg and Hammack (P.R. 75 1877 (1949)).

Another increase of the calculated cross sections could arise from the existence of exchange forces which tend to increase

calculations by a factor 1.5 to 2.0. The remaining difference, if any, may be removed by assuming a mechanism intermediate between that of direct one-step interaction as assumed here and evaporation from the nucleus as a whole, namely local heating of a portion of the nucleus and evaporation from the heated region before the excitation spreads over the whole nucleus.

The angular distribution of the (γ,p) process depends only on the angular momentum of the proton before and after the absorption. For dipole transitions $l \rightarrow l \pm 1$. The angular distribution is of the form $a + b \sin^2 \theta$ in the range of energy considered here; Levinger and Bethe [PR 78 115 (1950)] shown that dipole transitions are predominant.

$$I(\theta) \propto l(l+1) + \tfrac{1}{2}(l+1)(l+2)\sin^2\theta \quad \text{for} \quad l \rightarrow l+1$$

$$I(\theta) \propto l(l+1) + \tfrac{1}{2}\, l(l-1)\sin^2\theta \quad \text{for} \quad l \rightarrow l-1$$

This theory is also applicable to photoneutron production since the neutron effective charge is $-e\,Z/A$; it is therefore to be expected that the photoneutron spectrum will contain a low energy part due to evaporation and a high energy fraction containing a few percent of all the neutrons emitted with an anisotropic angular distribution.

Wilkinson's model (Proc. of the Glasgow Conference on Nuclear and Meson Physics (1954) p. 161)

The principal assumptions are:

1) The nucleus in the ground state is assumed to be fairly well described by the shell model.

2) In the excited state, we can also think in the existence of levels with a width $\Delta E \sim 3$ Mev. This estimate is done using the uncertainty principle.

$$\Delta E . \ \Delta t \sim h \qquad\qquad \Delta t = \frac{\lambda}{v}$$

where λ is the mean free path of the nucleon in the nucleus and v its velocity in the nucleus. It is well known that we can take.

$$\left.\begin{array}{l} \lambda \simeq 3\ R \\ R \simeq 10^{-12}\text{cm} \end{array}\right\} \quad \lambda \sim 3.10^{-12}\ \text{cm}$$

We can estimate

$$v = \sqrt{\frac{2E}{m}} \qquad \text{with} \quad E \sim 40 \text{ Mev}$$

So

$$\Delta E \simeq \frac{h}{3R}\sqrt{\frac{2E}{m}} = \frac{10^{-27}}{3.10^{-12}} \cdot \left(\frac{80.1,\ 6.10^{-6}}{1800.9.10^{-28}}\right) \sim 3 \text{ Mev}$$

3) The incoming photon interacts with only one nucleon, as in Courant's model, and rises it to an excited state where there is a probability $\neq 1$ (<u>here is the difference from Courant's model</u>) for decaying by the direct process or interacting with the rest of the nucleons leaving the nucleus in an excited collective state which decays in the manner described by the statistical theory.

4) Among all the possible El transitions, some are enhanced, especially these for which we have $\ell \longrightarrow \ell + 1$.

In the most extreme Wilkinson model, (only $\ell \rightarrow \ell + 1$ transitions) one expects an angular distribution of the type $A + B \sin^2 \theta$ where

$$\frac{B}{A} = \frac{1}{2} \left(1 + \frac{2}{\ell}\right)$$

So for ℓ very large

$$\frac{B}{A} \longrightarrow \frac{1}{2}$$

Systematic measurements of the angular distribution of fast photoneutrons were made by the Betatron group of the U.S.P. (Franca Tagliabue and J. Goldemberg) and it seems that, within experimental errors the neutrons of most of the elements (except Bi, Au, Pb, and D) are isotropic or show a very weak anisotropy.

::*:*:*:*:*

V. ELASTIC SCATTERING

1. Elastic Scattering in the Giant Resonance Region

The relationship between the total photonuclear and the photoneutron cross-sections can be seen in the following figure:

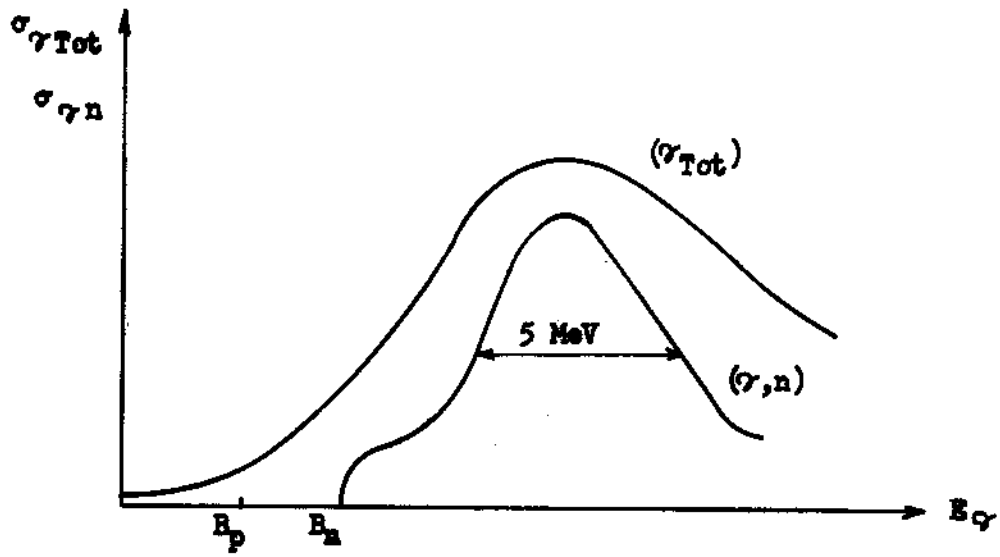

Fig. 20

For low energies sharp levels are known to exist in nuclei and correspondingly sharp peaks are found in the $\sigma_{\gamma Tot}$ (not shown in the figure). It is not known with certainty, however, whether the giant resonance is smooth or is composed of sharp, discrete levels. Information may be gathered from the comparison of experimental results on γ scattering with theoretical predictions on cross-sections and angular distributions.

Although no complete measurements are available on angular distributions for the giant resonance an E1 transition may be assumed, giving symmetry around 90°:

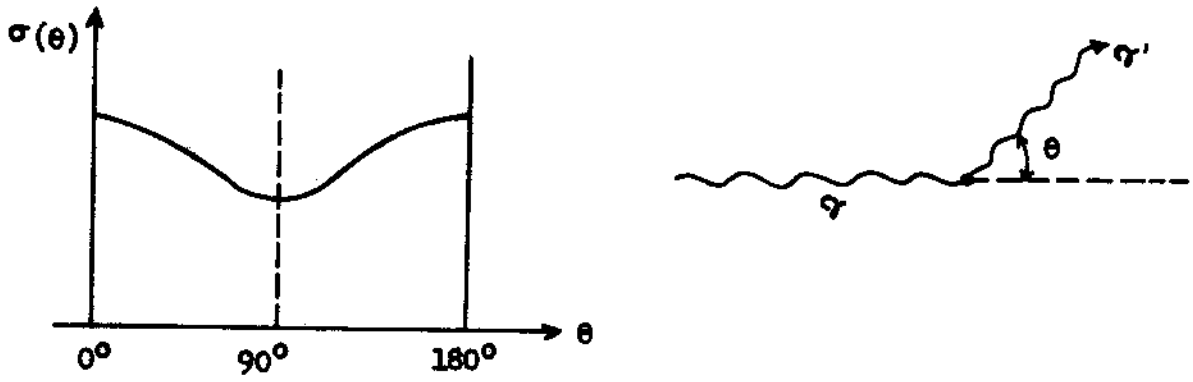

Fig. 21

For elastic γ-ray scattering on a single level we may write the resonance formula:

$$\sigma_{\gamma\gamma} = \pi \lambda^2 \cdot \frac{(2 J_{exc} + 1)}{2(2 J_{gr} + 1)} \cdot \frac{\Gamma_\gamma^2}{(E - E_0)^2 + \frac{\Gamma^2}{4}}$$

and for the total absorption cross-section:

$$\sigma_{\gamma Tot} = \pi \lambda^2 \cdot \frac{(2 J_{exc} + 1)}{2(2 J_{gr} + 1)} \cdot \frac{\Gamma_\gamma \Gamma}{(E - E_0)^2 + \frac{\Gamma^2}{4}}$$, where Γ

is the total level width and Γ_γ is the radiative width.

If we now assume $J_{gr} = 0$ and dipole interaction ($J_{exc} = 1$), these expressions reduce to the form:

$$\sigma = \frac{3\pi \lambda^2}{2} \cdot \frac{\Gamma_\gamma \Gamma}{(E - E_0)^2 + \frac{\Gamma^2}{4}}$$

where for each case the appropriate Γ must be inserted.

At $E = E_0$ we then have the maximum cross section

$$(\sigma_{\gamma\gamma})_{res} = \frac{(\sigma^2_{\gamma Tot})_{res}}{6\pi\lambda^2}$$

These expressions will be valid for single-level resonance or for non-interfering single levels, if average values are be taken for the Γ's.

For example for Cu, $\sigma_{\gamma Tot} = 200$ mb at resonance and $6\pi\lambda^2 \sim 23$ b at 17 Mev

$$\therefore (\sigma_{\gamma\gamma})_{res} \simeq \frac{(0.2 \text{ barn})^2}{(20 \text{ barn})} = 2 \text{ mb}$$

We can also write $(\sigma_{\gamma\gamma})_{res} = 6\pi\lambda^2 \left(\Gamma_\gamma/\Gamma\right)^2$ and if $\Gamma_\gamma = \Gamma$ (that is, at energies below particle emission thresholds and neglecting inelastic scattering) $(\sigma_{\gamma\gamma})_{res} \rightarrow 6\pi\lambda^2 \approx 23$ barn at 17 Mev. This result has been derived assuming that there is no particle emission and thus $6\pi\lambda^2$ represents the maximum possible value of the cross-section for elastic γ-ray scattering.

In the case of the carbon resonance at 15.1 Mev, $\sigma_{max} \sim 30$ barns, while experimentally the σ will be lowered because of Doppler broadening of resonance.

In general

$$(\sigma_{\gamma\gamma})_{res} = 6\pi\lambda^2 \left(\frac{\Gamma_\gamma}{\Gamma}\right)^2$$

So we can calculate Γ_γ : if $\sigma_{\gamma\gamma} \sim 2$ mb, $\Gamma \sim 5$ Mev and $6\pi\lambda^2 \sim 20$ b

$$\Gamma_\gamma = 5 \text{ Mev} \times \sqrt{\frac{0.002}{20}} = 5 \times 10^6 \times \sqrt{10^{-4}} = 50 \text{ Kev}$$

It follows that Γ_γ/Γ is of order 10^{-2}.

Elastic γ-ray scattering has been investigated experimentally by Fuller and Hayward at N.B.S. (Phys. Rev. 101, 692). Their maximum betatron energy was 40 Mev and the scattered photons were detected at 120° with a NaI(TI) crystal. Aluminium was used in the incident and scattered beams to remove low-energy photons (Fig. 24). Only the upper tip (about 1 Mev) of the bremsstrahlung

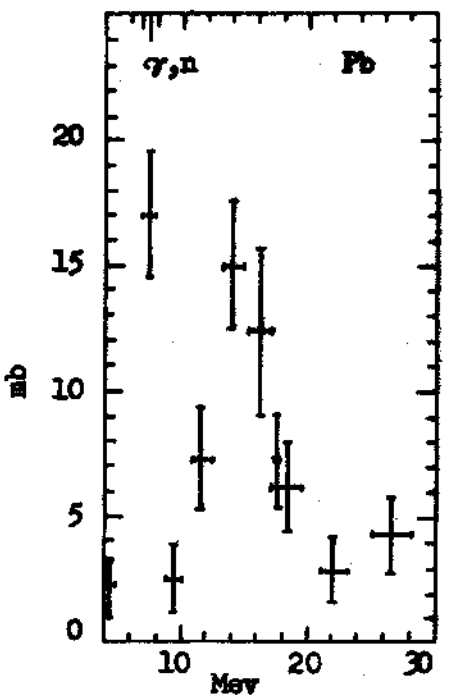

Fig. 22

spectrum was used for the cross section measurements and the background was low. Maximum counting rates of 20 per hour were achieved, limited by the duty cycle of the betatron.

Strong scattering peaks below particle emission thresholds have been observed in Na, Al, Mn, Ni, Sn, Pb, Bi and other elements. Above the particle emission thresholds the cross-section

goes through a maximum which for A > 50 resembles the g. r. in the (γ, n) cross-section. For A < 50 the curves are broader and peak at higher energies than the (γ, n) curve. The dependence on mass number of the energy at maximum of $\sigma(\gamma,\gamma)$ in the g. r. region is $E_m = 82\ A^{-1/3}$, which can be explained with a hydrodynamical model (Steinwedel-Jensen).

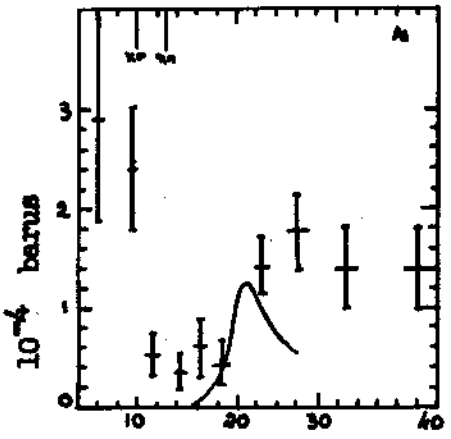

Fig. 23

Figures 22 and 23 reproduce the data on Pb and on Al. The solid curve in the latter figure correponds to the prediction of dispersion theory, as is explained below while low energy scattering is due to resonance fluorescence. Scattering associated with electronic processes is negligible in the experiment and only scattering by nuclei need be considered. There is a discrepancy which is appreciable on the high side of the giant resonance. In a more recent experiment, Penfold and Garwin (P.R. 116, 120) found reasonable agreement between experimental and calculated cross-section for C^{12} and Cu^{63} but not for O^{16}. (Fig. 25).

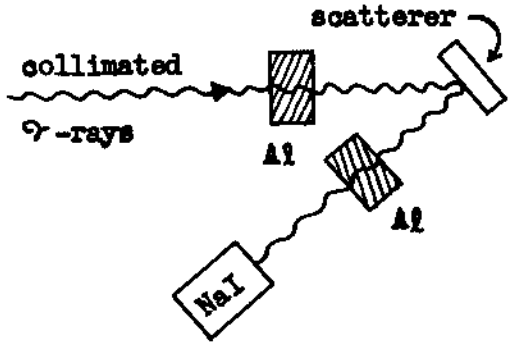

Fig. 24

The relationship between $\sigma_{\gamma\gamma}$ and $\sigma_{\gamma Tot}$ can be found more precisely by dispersion relation techniques. This has been

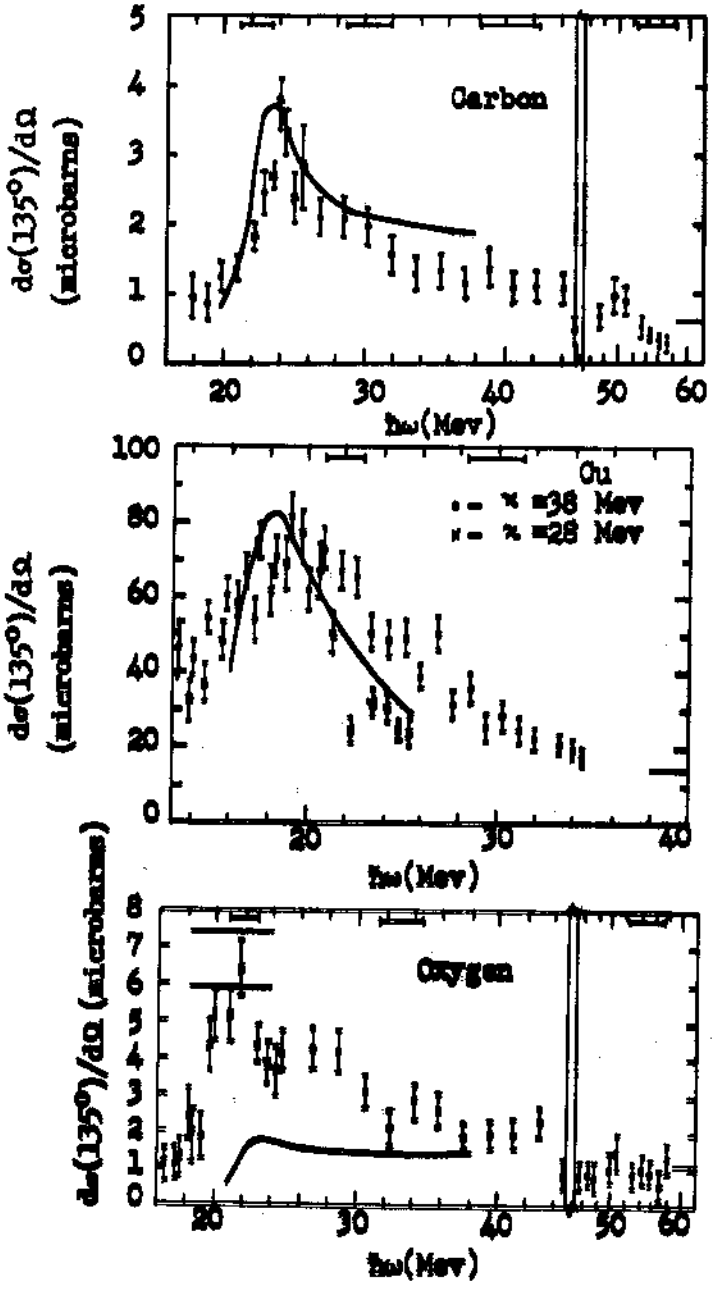

Fig. 25

done by Gell-Mann, Goldberger and Thirring (Phys. Rev. 95, 1612)

$$\sigma_{\gamma\gamma}(E) = \frac{1}{6\pi\lambda^2}\left[\sigma^2_{\gamma tot}(E) + \frac{2E_\gamma}{\pi} \cdot P\int\frac{\sigma_{\gamma tot}(E')dE'}{E'^2 - E^2}\right] + \sigma_{Thomp} +$$

$$+\sqrt{\sigma_{Thomp}}\cdot\sqrt{\frac{8}{3\pi}}\cdot\frac{1}{\pi hc}\cdot E^2\ P\int\frac{\sigma_{\gamma tot}(E')\,dE'}{E'^2 - E}$$

(P stands for Cauchy principal value).

The integrals are ~ 0 near the maximum. Near the peak of the giant resonance the dispersion relation reduces to

$$\sigma^2_{\gamma\,tot} = 6\pi\lambda^2(\sigma_{\gamma\gamma} - \sigma_{Thomp})$$

σ_{Thomp} is small $\sim \mu$ barns so it can be neglected and we get $\sigma^2_{\gamma tot} = 6\pi\lambda^2\sigma_{\gamma\gamma}$ as obtained before.

Out of resonance however, the other terms must be taken into account.

In practice the measured values are averages of this expression over bands of 1 - 2 Mev. In the region of the giant resonance average values may be used. Fuller and Hayward compared experimental results with this relation using $\sigma_{\gamma tot} \approx (\sigma_{\gamma n} + \sigma_{\gamma p})$ for the case of Aluminium, fig. 23. They found values for

$$\frac{(\sigma_{\gamma tot})^2}{\sigma_{\gamma\gamma}} \sim 6\pi\lambda^2$$

at resonance, but more scattering than expected at higher energies indicating some structure. Experiments have been carried out at the N.B.S. on deformed nuclei (Ta, Ho, Er) and spin effects

discussed by Baldin have been looked for.

The classical hydrodynamical picture seems to be adequate for the description of the giant resonance in the (γ,γ) cross-section. There is little evidence of fine structure in heavy nuclei.

2) Scattering of gamma rays in the energy region below the neutron threshold.

When we consider the interaction of γ-rays with matter in the energy region below the neutron threshold, rather narrow peaks can be observed in the total cross section excitation function due to sharp resonances at individual energy levels.

We are interested in considering the γ-γ cross-section contribution to these peaks. This process consists of an excitation of the nucleus by γ-absorption and re-emission, going again to the ground state. The width depends on the multipolarity of the radiation involved and have been expressed by the following relations:

for E1 $\Gamma_\gamma = \frac{0.22}{2J+1} \times A^{2/3} \times E^3 \sim$ 1000 eV (for 15 Mev)

for M1 $\Gamma_\gamma = 0.0033 \times E^3 \sim$ 100 eV " " "

for E2 $\Gamma_\gamma = 6 \times 10^{-6} \times E^5 \sim$ 1 eV " " "

There are also other contributions to the level width by the Doppler effect, due to thermal motion and due to the recoil of the nucleus during the emission process.

If E is the energy of the transition, and E' is the measured γ-ray energy, the Doppler shift is:

$$\delta = E - E', \text{ where}$$

$$E' = E \frac{1 + \beta\cos\theta}{\sqrt{1-\beta^2}} \simeq E(1 + \cos\theta) \quad \text{because } v \text{ is small}$$

with $\beta = \frac{v}{c}$ and $v \sim \sqrt{\frac{2kT'}{M}}$ (v velocity of recoiling nucleus, k Boltzmann constant, T' is the effective temperature which takes account of the vibrations of the scatterer atoms due to their binding in a chemical lattice, M mass of nucleus).

To see the magnitude of this effect we can calculate the Doppler broadening δ for the 15.1 Mev (M1) transition in C^{12}. One finds that for carbon $T' = 450^{\circ}K$. The Doppler broadening due to thermal motion is $\delta \sim 50$ eV. with a Gaussian shape. Measurements of Γ_γ are always modified by this effect.

There are several possible ways to study experimentally the gamma ray scattering process.

A bremsstrahlung beam from a betatron is conveniently collimated, monitored and allowed to interact with a carbon scatterer. The radiation may the attenuated by a carbon absorber and the scattered γ-rays are detected by a scintillation spectrometer (Garwin, Phys. Rev. 114, 143 (1959)). The experimental arrangement is as follows.

If the angular distribution of the scattered photons is plotted, it shows that the experimental points fit accurately

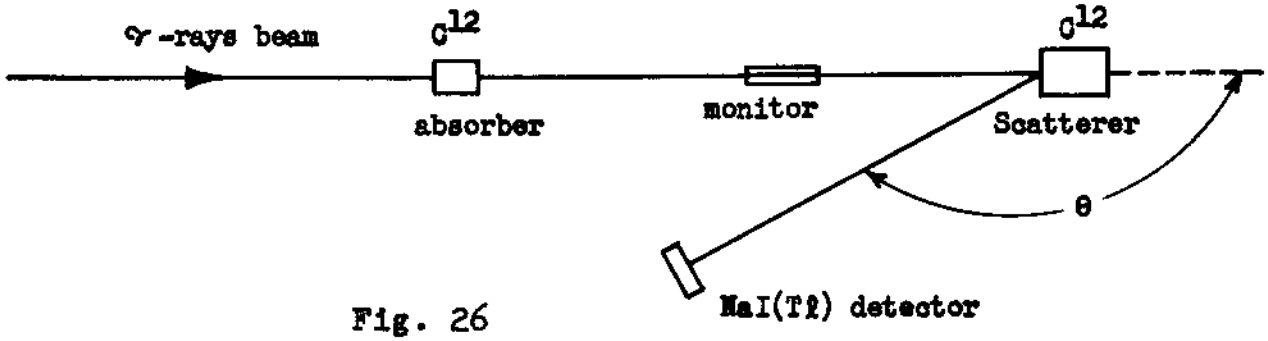

Fig. 26

the distribution $(1 + \cos^2 \theta)$, corresponding to dipole transitions.

When the pulse height distribution obtained in the elastic scattering of 15.1 Mev γ-rays is studied one notices that after subtracting the conventional background, there still remains the so called non resonant contribution to scattering. This contribution is not strongly affected by the absorber in the main beam, and grows linearly with the scatterer thickness.

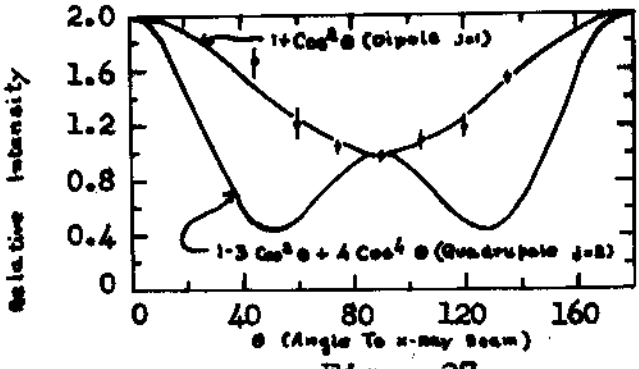

Fig. 27

The Self-absorption Experiment

This consists in observing the attenuation of the scattered

γ-rays when carbon absorbers are placed in the incident beam.

The yield of scattered photons is measured as a function of the thickness of the absorber. Calculations are then made using Breit and Wigner absorption formulas for several values of δ/Γ using a X^2 test to find the best fit of data to theory. One obtains

$$\frac{\delta}{\Gamma} = 0.59 \pm 0.12$$

and this implies a value of $\sigma_n^o = 29.7 \pm 1.1$ barn. Since for a dipole transition

$$\Gamma_\gamma/\Gamma = \sigma_n^o / 6\pi\lambda^2 = 0.92 \pm 0.034 \quad \text{then} \quad \Gamma = 67 \pm 14 \text{ eV}.$$

The Production Experiment

The production experiment consists in studying the growth in the number of 15.1 MeV γ's as a function of scatterer thickness. An yield curve A(T) is then obtained.

Calculated curves of $\log A(T)/\delta$ versus $\log (T\sigma_n^o \Gamma/\delta)$ for various δ/Γ are available:

Assuming $\sigma_n^o = 29.7$ barns and using a X^2 fit one obtains a value of $\delta/\Gamma = 0.67 \pm 0.16$ in agreement with the one obtained by the first method.

Integrated scattering cross section

The number of γrays scattered from a target of a given thickness T is closely related to the integrated cross section, the

solid angle and efficiency of the NaI detector. Knowing those quantities one obtains $I=\int \sigma\, dE = 2.11 \pm 0.31$ mb. Mev.

From the data obtained by the three methods after averaging one gets

$$\sigma_n^o = 29.7 \pm 1.1 \text{ barns.} \qquad \Gamma_\gamma = 59.2 \pm 9.7 \text{ eV}$$

$$\delta/\Gamma = 0.62 \pm 0.10 \qquad I = 2.33 \pm 0.19 \text{ mb Mev}$$

$$\Gamma = 64.5 \pm 10.4 \text{ eV}$$

D. Kurath (Phys. Rev. 106, 975 (1957) has calculated for the width of the 15.1 Mev transition the value 54.5 ± 9.3 eV., in reasonable agreement. The width of the first excited level is found to be about 4 eV., but this value is only approximate, because of the uncertainty of branching ratios.

Also, the radiation width to the first excited state of C^{12} has been determined by the branching ratio of this transition, resulting 3.2 ± 2.5 eV.

A systematic investigation of the average scattering of 6-7 Mev gamma rays has been made by Reibel and Mann at the University of Pennsylvania who find scattering cross sections systematically increasing with atomic number.

Other individual resonances have been studied in detail by Cohen and Tobin with the Naval Research Laboratory betatron. A good survey of other studies of resonance scattering has been presented by F. Metzger in Progress of Nuclear Physics (1959).

Recoilless scattering found by Mossbauer is an extreme example of resonance scattering. A report on a recent conference on Mossbauer Scattering by Frauenfelder and Lustig is available from the University of Illinois (June 1960).

::*:*:*:*:*

VI - POLARIZED BREMMSTRAHLUNG

In order to investigate the polarization of bremmstrahlung γ-rays and decide on the electric or magnetic character of the dipole 15.1 MeV level in C^{12}, a detailed experiment has been recently performed (D. Jamnik and P. Axel, University of Illinois (1960) using a 25 MeV electron beam. Bremmstrahlung was produced on a thin internal target with the experimental set-up as the indicated below

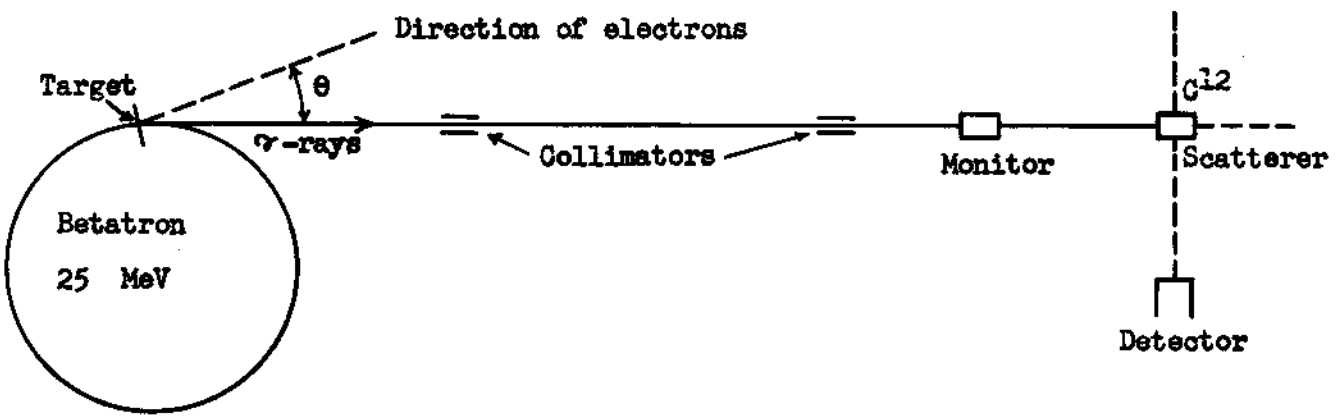

Fig. 28

In bremmstrahlung processes, the production plane is defined by the directions of the incident electron and the emerging photon as shown.

This plane is sharply defined only when an infinitely thin target is considered, because of the possibility of electrons radiating after being scattered inside the target. In this case, the distribution of radiating electrons after multiple or simple

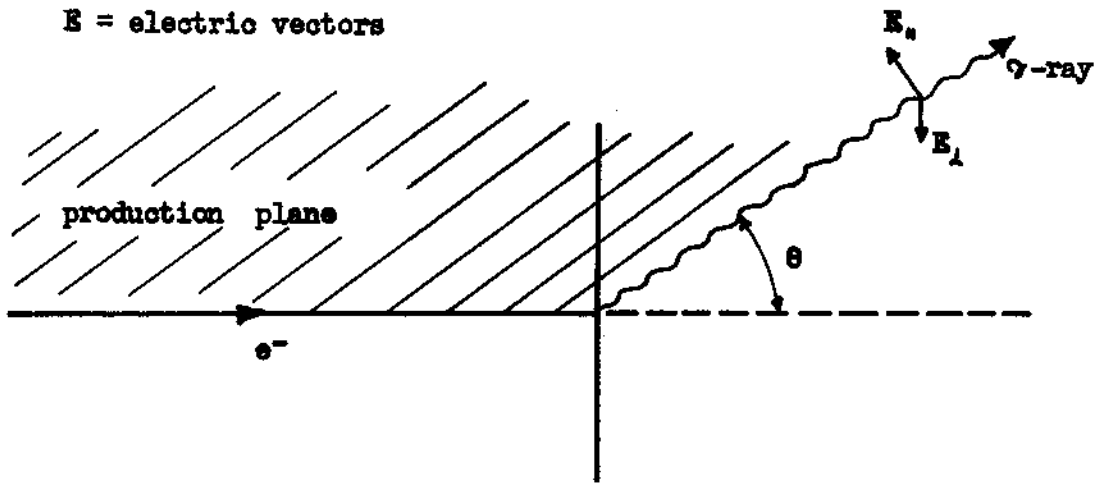

Fig. 29

scattering in the target must be taken into account.

If I_{11} and I_1 are the photon intensities with electric vectors E_{11} and E_1 paralell and normal to the production plane the polarization is defined by

$$\pi = \frac{I_1 - I_{11}}{I_1 + I_{11}}$$

It is more convenient to use the expression

$$P = \frac{I_1}{I_{11}} = \frac{1+\pi}{1-\pi}$$

P is a function of the incident electron energy, E_e, the emitted photon energy, E_γ and the angle between their directions, θ. As a function of E_γ, P increases as E_γ decreases. As a function of θ, P = 1 for $\theta = 0$ and has a maximum value for $\theta = mc^2/E_e$ (where m is the electron rest mass).

a) Properties of the 15.1 Mev in C^{12}.

For 15.1 Mev photons produced by 25 Mev electrons on Al target with negligible thickness, the theory gives P = 1.83 (for $\theta = \theta_o = 0.02$ radians). If the target has a thickness of 30 mg/cm^2, then P = 1.35 for $\theta = \theta_o$ and grows to P = 1.47 for $\theta = 1.6\ \theta_o$. The predictions of theory are shown in the next graph.

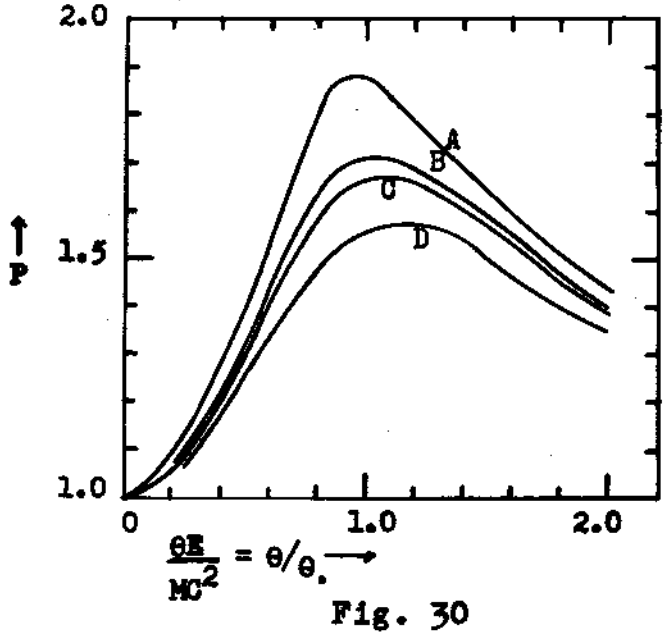

Fig. 30

In the detailed experience that we are considering, the production plane was horizontal and the detector could rotate on a plane normal to the main γ-beam. The angle θ could be changed by shifting the target on the betatron beam. P can be determined by comparing the number of photons scattered perpendicular to the production plane N_1 to the number scattered in the production plane N_{11}. If the scattering were a pure electric dipole process I_1 could contribute only to N_{11} but not to N_1.(This corresponds to the classical fact that an oscillating charge does not radiate in the direction of its acceleration). Similarly I_{11}

would contribute only to N_1. For a magnetic dipole scattering process I_1 contributes only to N_1 while I_{11} contributes to N_{11}.

The angular distribution of photons in the detector plane (perpendicular to the propagation of the photons) when the detector is rotated and θ kept fixed has been measured in this experiment, the result is shown in fig. 31.

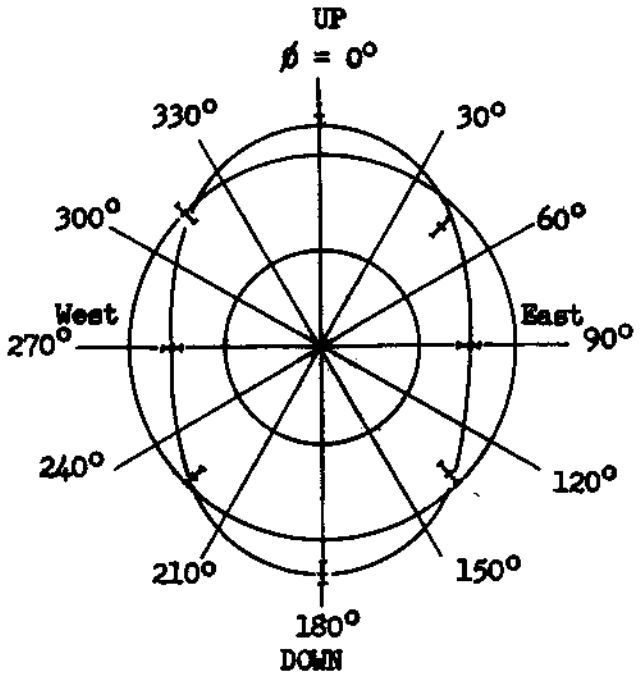

Fig. 31

This shows that $N_1/N_{11} > 1$; then, the scattering level is M1. The ground state of C^{12} is known to be 0^+. Then, the 15.1 Mev level is 1^+.

b) Investigation of polarization as a function of θ and Z.

The polarization was investigated changing the angle θ and measuring counts in the production plane and perpendicular

to it, and calculating the polarization.

The results were compared with the theory, showing a reasonable agreement within the experimental difficulties and theoretical approximations involved.

The comparison is shown in fig. 32.

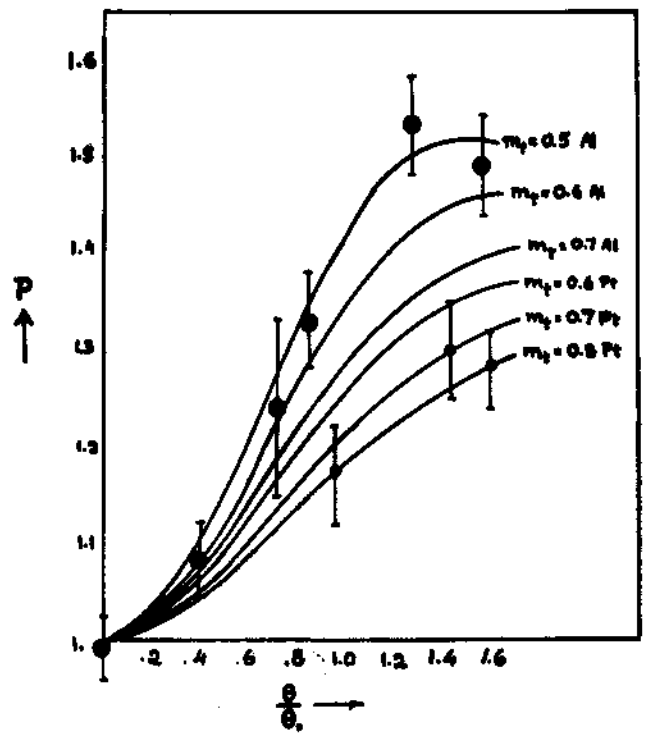

Fig. 32

m is a measure of the thickness of the target and is defined by

$$m = 4.5 \times 10^{-2} \times \frac{Z}{\sqrt{A}} \cdot \sqrt{t}$$

where t is measured in mg/cm^2, Z and A are the atomic and mass numbers.

c) Investigation of the tip of bremmstrahlung at the high frequency limit.

The elastic scattering of 15.1 Mev by C^{12} was used to measure the tip of bremmstrahlung spectrum changing the maximum energy of the electrons (isocromat) from -15.12 Mev to -17.5 Mev.

The form of the tip of bremmstrahlung spectrum has been checked for several targets and the results are shown in fig. 33. As it can be seen the theory based on Born approximation fits the experimental data for low Z, but does not account for the results when Z increases.

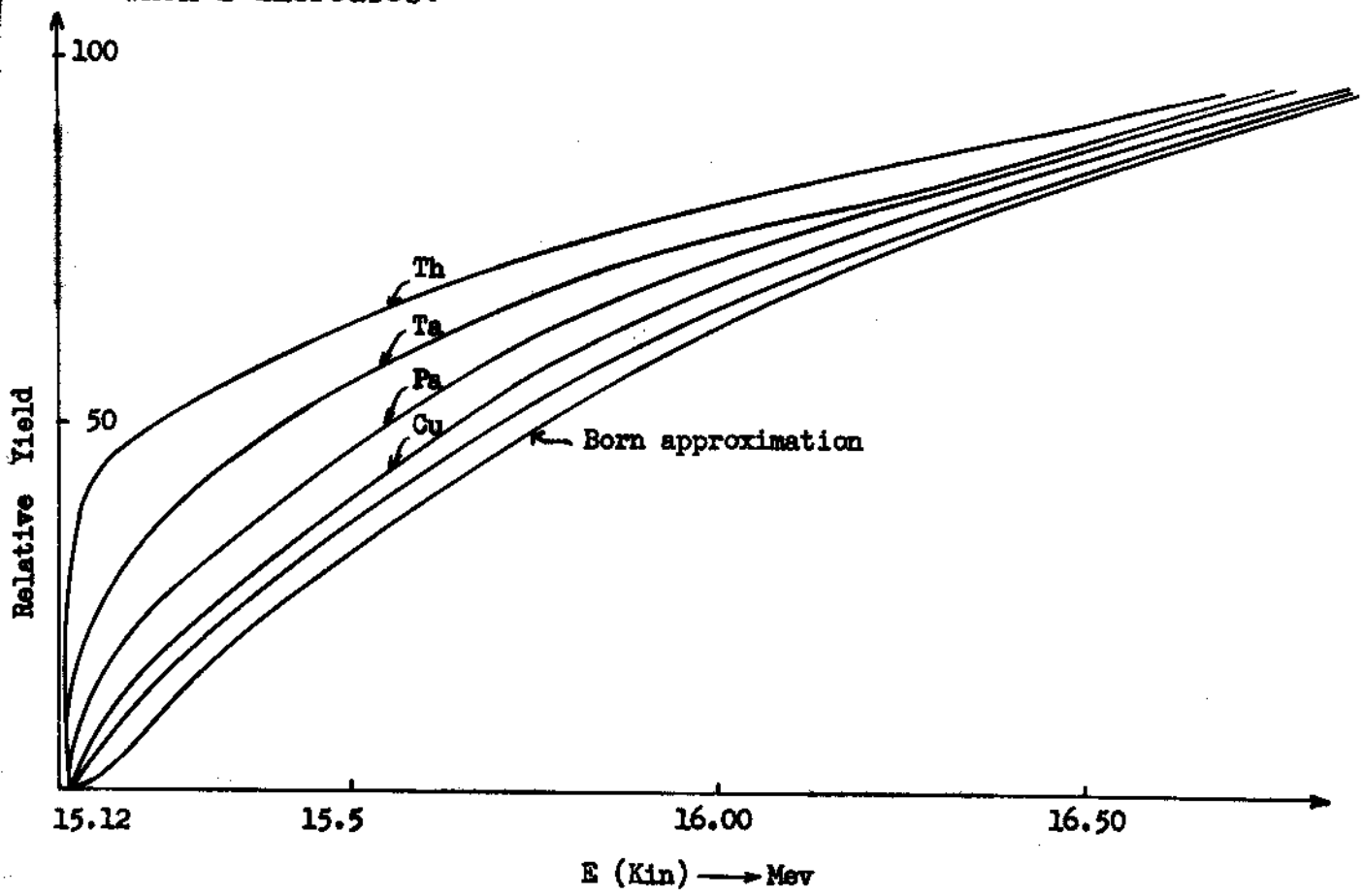

Fig. 33

A qualitative explanation of the results has been made by Fano et al. who relate the bremmstrahlung at the limit to the photoeffect by detailed balance. This theory predicts a yield at the limit which varies as $Z^{2.7}$ while the experimental results indicate a $Z^{3.5 \pm 0.1}$ dependence.

The polarization of the radiation was investigated but none was found with the limits of error $\sim$ 10%.

::*:*:*:*:*:*:*